Secreted protein Del-1 regulates myelopoiesis in the hematopoietic stem cell niche

Ioannis Mitroulis,[1] Lan-Sun Chen,[1] Rashim Pal Singh,[1] Ioannis Kourtzelis,[1] Matina Economopoulou,[2] Tetsuhiro Kajikawa,[3] Maria Troullinaki,[1] Athanasios Ziogas,[1] Klara Ruppova,[1] Kavita Hosur,[3] Tomoki Maekawa,[3] Baomei Wang,[3] Pallavi Subramanian,[1] Torsten Tonn,[4] Panayotis Verginis,[1,5] Malte von Bonin,[6] Manja Wobus,[6] Martin Bornhäuser,[6,7] Tatyana Grinenko,[1] Marianna Di Scala,[8] Andres Hidalgo,[8,9] Ben Wielockx,[1,7] George Hajishengallis,[3] and Triantafyllos Chavakis[1,7]

[1]Department of Clinical Pathobiochemistry, Institute for Clinical Chemistry and Laboratory Medicine, and [2]Department of Ophthalmology, University Hospital Carl Gustav Carus, Technische Universität Dresden, Dresden, Germany. [3]Department of Microbiology, Penn Dental Medicine, University of Pennsylvania, Philadelphia, Pennsylvania, USA. [4]Institute for Transfusion Medicine, German Red Cross Blood Donation Service North-East, Dresden, Germany. [5]Biomedical Research Foundation of the Academy of Athens, Athens, Greece. [6]Medical Clinic and Policlinic I, University Hospital Carl Gustav Carus, Technische Universität Dresden, Dresden, Germany. [7]Center for Regenerative Therapies Dresden, Dresden, Germany. [8]Area of Cell and Developmental Biology, Fundación Centro Nacional de Investigaciones Cardiovasculares (CNIC) Carlos III, Madrid, Spain. [9]Institute for Cardiovascular Prevention, Ludwig-Maximilians-Universität München, Munich, Germany.

Hematopoietic stem cells (HSCs) remain mostly quiescent under steady-state conditions but switch to a proliferative state following hematopoietic stress, e.g., bone marrow (BM) injury, transplantation, or systemic infection and inflammation. The homeostatic balance between quiescence, self-renewal, and differentiation of HSCs is strongly dependent on their interactions with cells that constitute a specialized microanatomical environment in the BM known as the HSC niche. Here, we identified the secreted extracellular matrix protein Del-1 as a component and regulator of the HSC niche. Specifically, we found that Del-1 was expressed by several cellular components of the HSC niche, including arteriolar endothelial cells, CXCL12-abundant reticular (CAR) cells, and cells of the osteoblastic lineage. Del-1 promoted critical functions of the HSC niche, as it regulated long-term HSC (LT-HSC) proliferation and differentiation toward the myeloid lineage. Del-1 deficiency in mice resulted in reduced LT-HSC proliferation and infringed preferentially upon myelopoiesis under both steady-state and stressful conditions, such as hematopoietic cell transplantation and G-CSF– or inflammation-induced stress myelopoiesis. Del-1–induced HSC proliferation and myeloid lineage commitment were mediated by β3 integrin on hematopoietic progenitors. This hitherto unknown Del-1 function in the HSC niche represents a juxtacrine homeostatic adaptation of the hematopoietic system in stress myelopoiesis.

Introduction

Hematopoietic stem cells (HSC) lie at the core of the hematopoietic and immune systems and have a unique capacity for self-renewal and differentiation to multipotent and lineage-committed hematopoietic progenitors, which give rise to mature cells of the myeloid and lymphoid lineages (1). Under steady-state conditions, HSCs remain mostly quiescent and have a limited function in the maintenance of hematopoiesis (1–3). However, HSCs promptly switch to a proliferative state in order to meet the increased demands in response to hematopoietic stress, such as bone marrow (BM) injury, transplantation, or systemic infection (1, 3). The specialized micro-anatomical environment in the BM in which HSCs reside is designated the HSC niche and crucially regulates the homeostatic balance between quiescence, self-renewal, and differentiation of HSCs. Recent advances in BM imaging reveal a perivascular distribution of HSCs in their niche, which comprises several cell populations. Endothelial (4–11) and perivascular stromal cells (9, 12–14), including CXCL12-abundant reticular cells (CAR cells) (15, 16), are considered the main cell populations constituting the homeostatic HSC niche, whereas osteolineage cells and osteoblasts have a significant role in the post-transplant HSC niche (3, 17, 18). Niche cells regulate HSC homeostasis through paracrine growth factor and chemokine signals as well as via adhesive interactions (3, 5, 9, 19, 20).

Therapies targeting HSCs, including the administration of growth factors such as granulocyte colony–stimulating factor (G-CSF) and HSC transplantation, have revolutionized the clinical outcome in patients with malignancies or BM failure syndromes (21, 22). G-CSF–based HSC mobilization is the main strategy used in both autologous and allogeneic transplantation (23). However, G-CSF administration fails to mobilize adequate numbers of HSCs for transplantation in a substantial number of healthy donors and patients (21, 23, 24), rendering the development of additional mobilization strategies imperative. Moreover, G-CSF is used as a prophylactic treatment in patients with increased risk for iatrogenic neutropenia (25, 26) and in the treatment of patients with congenital neutropenia (27, 28).

Developmental endothelial locus–1 (Del-1), a glycoprotein secreted by endothelial and certain other cells, becomes associated with the extracellular matrix or cellular surfaces and interacts with

Authorship note: I. Mitroulis, L.S. Chen, and R. Pal Singh contributed equally to this work as first authors. B. Wielockx, G. Hajishengallis, and T. Chavakis contributed equally to this work as senior authors.
Conflict of interest: The authors have declared that no conflict of interest exists.
Submitted: December 29, 2016; **Accepted:** July 11, 2017.
Reference information: *J Clin Invest*. 2017;127(10):3624–3639.
https://doi.org/10.1172/JCI92571.

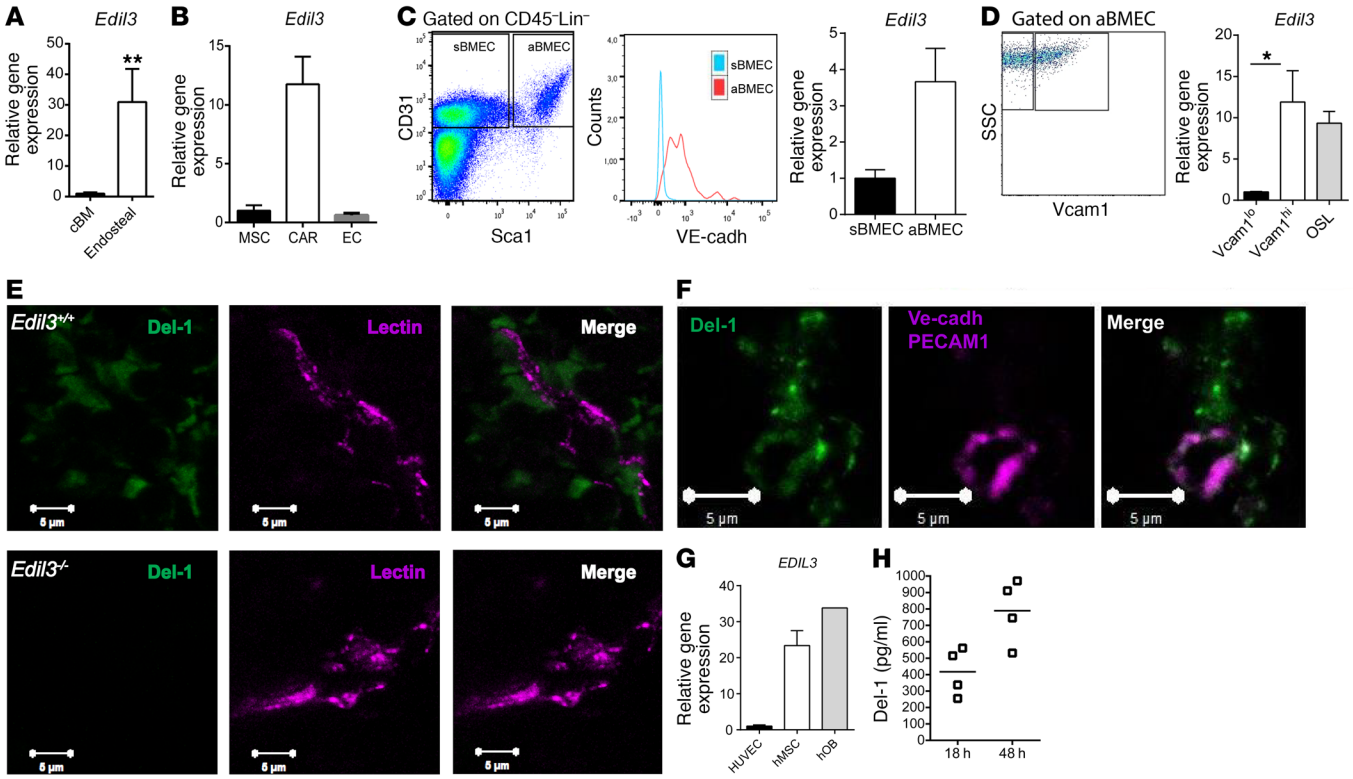

Figure 1. Expression of Del-1 in HSC niche cell populations. (**A**) *Edil3* mRNA levels in the cBM and endosteal region (n = 5 mice per group). (**B**) *Edil3* mRNA levels in stromal cell populations from CXCL12-GFP mice: CD45$^-$Ter119$^-$CD31$^-$GFP^{hi} (CAR) cells, CD45$^-$Ter119$^-$CD31$^-$GFP$^-$ MSCs, and CD45$^-$Ter119$^-$CD31$^+$GFP^{int} endothelial cells (EC; n = 3–4). The mRNA expression was normalized against β2M. (**C**) Gating strategy for the isolation of endothelial cells. After gating on CD45$^-$Lin$^-$ cells, sinusoidal (sBMEC; CD31$^+$Sca1$^-$) and arteriolar (aBMEC; CD31$^+$Sca1$^+$) BM endothelial cells were isolated. VE-cadherin (VE-cadh) staining was used to confirm the arteriolar origin of the CD31$^+$Sca1$^+$ cell population. Right: *Edil3* mRNA levels in sBMECs and aBMECs (n = 3–4). mRNA expression was normalized against β2M. (**D**) aBMECs were further sorted according to Vcam1 expression. *Edil3* mRNA levels in Vcam1^{lo} and Vcam1^{hi} aBMECs as well as in CD45$^-$Lin$^-$CD31$^-$Sca1$^-$CD51$^+$ OSL cells (n = 4–5). mRNA expression was normalized against β2M. (**E**) Localization of Del-1 in the perivascular area of the BM; vessel lumen staining was performed with isolectin B4 (lectin). Del-1–deficient mice served as controls for the Del-1 staining. (**F**) Fluorescence microscopy image showing the presence of Del-1 in arterioles. Endothelial staining was performed using anti-PECAM1 and VE-cadherin antibodies. Scale bars: 5 µm. (**G**) *EDIL3* mRNA in hMSCs and primary human osteoblasts (hOB) was compared with *EDIL3* mRNA in HUVECs (HUVECs, n = 4 independent cultures; hMSCs, n = 4 donors; hOBs, n = 1 performed in technical replicates). The mRNA expression was normalized against GAPDH. (**H**) Del-1 concentration in culture supernatants of hMSCs was assessed by ELISA (n = 4 donors). Data are presented as mean ± SEM. Mann-Whitney U test, $^*P < 0.05$, $^{**}P < 0.01$.

integrin receptors (29–31). It consists of three N-terminal EGF-like repeats and two C-terminal discoidin I–like domains, and hence also is designated EGF-like repeats and discoidin-I–like domains–3 (EDIL3) (32). We have previously identified Del-1 as an endogenous modulator of leukocyte adhesion through interaction with integrin αLβ2 (LFA-1; CD11a/CD18) (29, 31). Moreover, Del-1 interacts with β3 integrin (CD61) via an Arg-Gly-Asp (RGD) motif on the second EGF-like repeat (30).

In the present work, we observed that Del-1 is expressed by several major cellular components of the HSC niche, though not by hematopoietic progenitors. In particular, Del-1 is expressed by those niche cells that have a major role in the maintenance of HSCs, i.e., arteriolar endothelial cells and perivascular CAR cells (3, 6, 7, 9, 15). In addition, Del-1 is expressed by cells of the osteoblastic lineage that crucially mediate the engraftment of HSCs in the post-transplantation niche (3, 17, 18). This spatial distribution of Del-1 raised the possibility that it might be involved in the regulation of hematopoiesis. We addressed this hypothesis using in vivo models of steady-state, regenerative, and stress hematopoiesis and in vitro mechanistic approaches. We show that Del-1, via its interaction with the αvβ3 integrin, promotes several critical functions in the niche, including HSC retention, hematopoietic progenitor cell cycle progression, and myeloid lineage commitment of HSCs. Del-1 thereby regulates myelopoiesis under steady-state conditions and in G-CSF– or inflammation-induced stress myelopoiesis, as well as myelopoiesis reconstitution under regenerative/transplantation conditions. Del-1 is hence a niche component that serves a juxtacrine homeostatic adaptation of the hematopoietic system in inflammation-related and regeneration myelopoiesis.

Results

Del-1 expression in the BM. First, we sought to investigate whether Del-1 is present in the BM. We initially studied the expression of the Del-1–encoding gene *Edil3* in the BM niche and hematopoietic cell populations. We found that *Edil3* mRNA expression was significantly higher in the endosteal region as compared with the central BM (cBM) (Figure 1A), suggesting that Del-1 is enriched at the endosteal area of the BM. Analysis of sorted cells from CXCL12-GFP mice (33, 34) demonstrated that *Edil3* was highly expressed

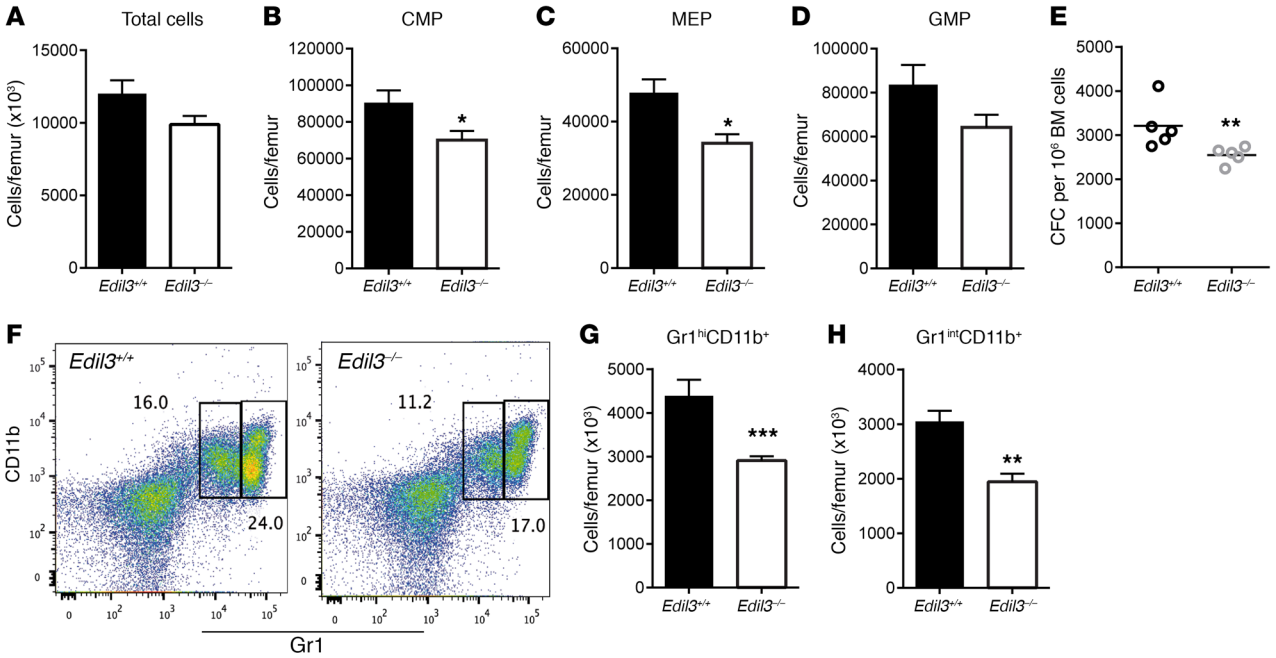

Figure 2. Del-1 supports myeloid lineage development. (**A**) Total BM cell numbers in the BM of 10-week-old *Edil3*$^{-/-}$ and *Edil3*$^{+/+}$ mice (n = 10 mice per group). (**B**) CMP, (**C**) MEP, and (**D**) GMP cell numbers in the BM of *Edil3*$^{-/-}$ (n = 13) and *Edil3*$^{+/+}$ mice (n = 14). (**E**) CFCs in the BM of *Edil3*$^{-/-}$ and *Edil3*$^{+/+}$ mice (n = 5 mice per group). (**F**) Representative flow cytometry plots and (**G**) Gr1^{hi}CD11b^{+} granulocyte and (**H**) Gr1^{int}CD11b^{+} myeloid cell numbers in the BM of 10-week-old *Edil3*$^{-/-}$ (n = 9) and *Edil3*$^{+/+}$ mice (n = 8). Data are presented as mean ± SEM. Mann-Whitney U test, $^{*}P < 0.05$, $^{**}P < 0.01$, $^{***}P < 0.001$.

in CAR cells (CD45^{-}TER119^{-}CD31^{-}GFP^{hi}) as compared with endothelial cells (CD45^{-}TER119^{-}CD31^{+} GFP^{int}) and CXCL12-negative stromal cells (Figure 1B). Furthermore, analysis of sorted BM endothelial cells demonstrated that *Edil3* is predominantly expressed in Lin^{-}CD45^{-}CD31^{+}Sca1^{+} arteriolar BM endothelial cells (aBMECs) as compared with Lin^{-}CD45^{-}CD31^{+}Sca1^{-} sinusoidal BM endothelial cells (sBMECs) (Figure 1C) (6). The expression of VE-cadherin by the Lin^{-}CD45^{-}CD31^{+}Sca1^{+} population further confirmed their arteriolar origin (Figure 1C) (6). Further analysis identified a Vcam1^{hi} subpopulation within the aBMECs expressing the highest *Edil3* mRNA levels (Figure 1D). Moreover, Del-1 was expressed by Lin^{-}CD45^{-}CD31^{-}Sca1^{-}CD51^{+}osteolineage (OSL) cells (Figure 1D). In contrast, *Edil3* mRNA expression could not be detected in multipotent progenitors (MPPs; Lin^{-}cKit^{+}Sca1^{+} CD48^{+}CD150^{-}), long-term HSCs (LT-HSCs) (Lin^{-}cKit^{+}Sca1^{+}CD48^{-} CD150^{+}), or other hematopoietic cell populations in the BM, such as Lin^{+} cells (data not shown). The spatial distribution of Del-1 in the perivascular area of the BM and its expression in the endothelium of BM arterioles (diameter approximately 5 μm; ref. 6) were verified by immunostaining (Figure 1, E and F, and Supplemental Figure 1. We further evaluated the expression of Del-1 in primary human BM-derived mesenchymal stromal cells (hMSCs) and primary human osteoblasts (hOBs) by quantitative PCR. *EDIL3* was highly expressed in hMSCs and hOBs, compared with HUVECs (Figure 1G), a cell population known to express substantial levels of *EDIL3* (31, 35). Del-1 protein was also detected in culture supernatants of primary hMSCs, further showing that Del-1 can be produced and released by stromal cells in the human BM microenvironment (Figure 1H). Thus, Del-1 is expressed in the BM by distinct niche cell populations that promote HSC maintenance under steady-state conditions, including endothelial cells (4–7) and perivascular stromal cells, like CAR cells, (9, 14–16), and by cells that mediate the reconstitution of hematopoiesis after transplantation, like OSL cells (3, 17, 18).

Del-1 promotes steady-state myelopoiesis. We next assessed whether Del-1 could affect hematopoietic progenitor maintenance and function. Specifically, to determine a possible functional role of Del-1 in the regulation of hematopoiesis, we performed BM analysis in adult Del-1–deficient (*Edil3*$^{-/-}$) and Del-1–proficient (WT; *Edil3*$^{+/+}$) mice. Although Del-1 deficiency had no significant effect on total BM cellularity (Figure 2A), it caused a significant decrease in the number of common myeloid progenitors (CMPs; Lin^{-}cKit^{+} Sca1^{-}CD16/32^{-}CD34^{+}) (Figure 2B) and megakaryocyte erythrocyte progenitors (MEPs; Lin^{-}cKit^{+}Sca1^{-}CD16/32^{-}CD34^{-}) (Figure 2C). The numbers of granulocyte macrophage progenitors (GMPs; Lin^{-}cKit^{+}Sca1^{-}CD16/32^{+}CD34^{+}) were not significantly decreased in the BM of *Edil3*$^{-/-}$ mice as compared with *Edil3*$^{+/+}$ mice (Figure 2D). Moreover, the use of a CFU assay revealed decreased numbers of functional progenitor cells (colony-forming cells [CFCs]) in the BM of *Edil3*$^{-/-}$ mice, as compared with *Edil3*$^{+/+}$ mice (Figure 2E). The decrease in myeloid progenitor cells was associated with a significant decrease in the numbers of Gr1^{hi}CD11b^{+} granulocytes (Figure 2, F and G) and Gr1^{int}CD11b^{+} myeloid cells (Figure 2, F and H) in the BM of *Edil3*$^{-/-}$ mice as compared with *Edil3*$^{+/+}$ mice. In contrast, no difference was observed in the levels of G-CSF in peripheral blood (Supplemental Figure 2), in the number of different B cell populations, or in the numbers of common lymphoid progenitors (CLPs; Lin^{-}Sca1^{lo}cKit^{lo}Flt3^{+}IL7Rα^{+}) in the BM due to Del-1 deficiency (Supplemental Figure 3). Since steady-state hematopoiesis is maintained by long-lived multipotent progenitors (2), we studied whether Del-1 deficiency had a quantitative and/or a qualitative effect on hematopoietic progenitors. No difference was seen in the

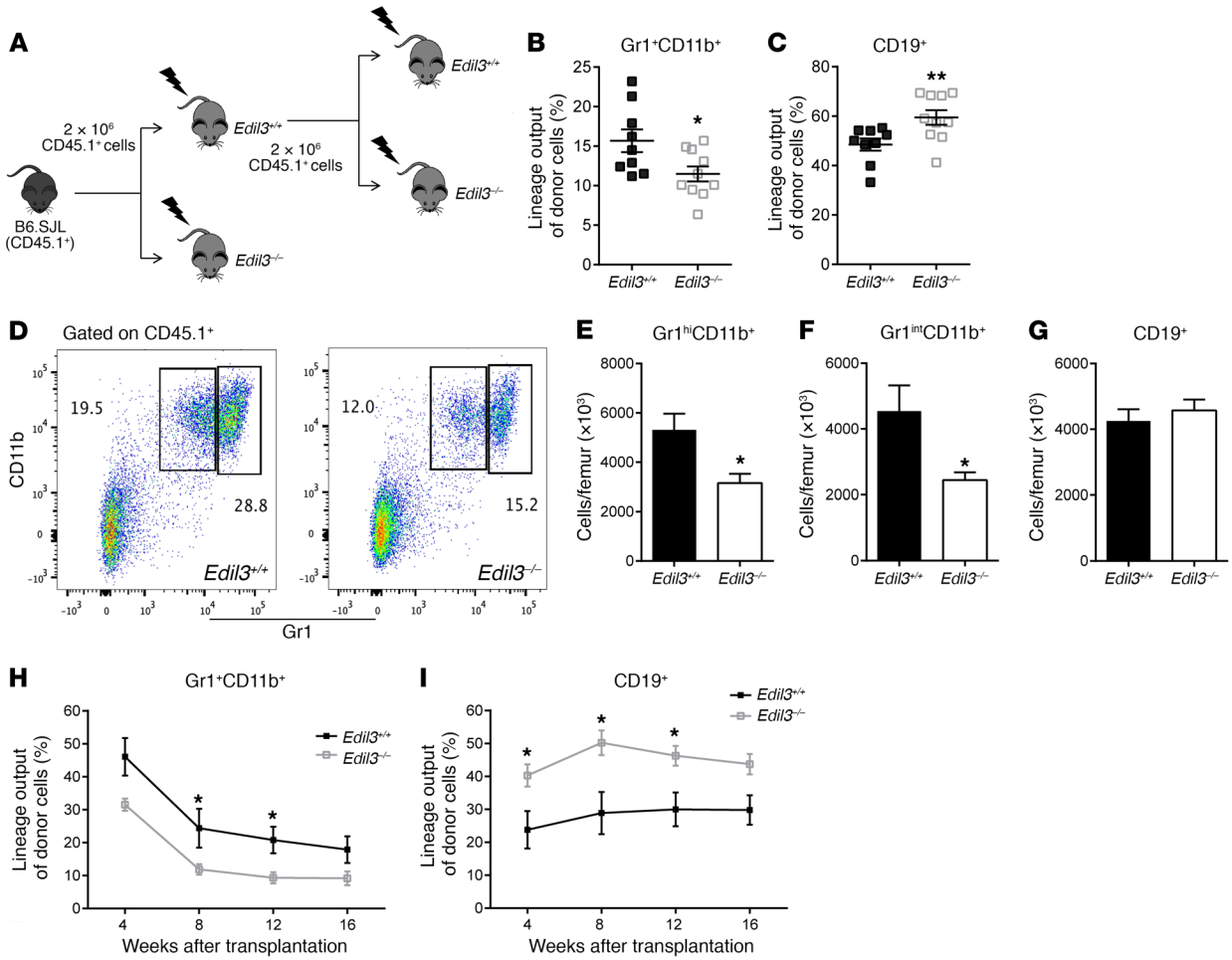

Figure 3. Del-1 promotes regeneration of myelopoiesis. (**A**) Experimental design used to study the effect of Del-1 expressed in the BM of recipient mice on the long-term development of myelopoiesis upon hematopoietic cell transplantation. Lethally irradiated *Edil3*$^{+/+}$ or *Edil3*$^{-/-}$ mice (CD45.2) were transplanted with CD45.1$^+$ BM cells, as described in Methods. (**B**) Percentage of Gr1$^+$CD11b$^+$ myeloid and (**C**) CD19$^+$ B cells in donor-derived cells in the peripheral blood of *Edil3*$^{-/-}$ (n = 10) and *Edil3*$^{+/+}$ recipient mice (n = 9) at 16 weeks after transplantation. (**D**) Representative flow cytometry plots; (**E**) donor-derived Gr1^{hi}CD11b$^+$ granulocytes, (**F**) donor-derived Gr1^{int}CD11b$^+$ myeloid cells, and (**G**) donor-derived CD19$^+$ B cells in the BM of recipient *Edil3*$^{-/-}$ (n = 10) or *Edil3*$^{+/+}$ (n = 9) mice 16 weeks after transplantation. (**H**) Percentage of Gr1$^+$CD11b$^+$ myeloid and (**I**) CD19$^+$ B cells in donor-derived cells in the peripheral blood of *Edil3*$^{-/-}$ (n = 10) and *Edil3*$^{+/+}$ recipient mice (n = 8) at different time points after secondary transplantation. Data are presented as mean ± SEM. Mann-Whitney U test, $^*P < 0.05$, $^{**}P < 0.01$.

numbers of LSK (Lin$^-$Sca1$^+$cKit$^+$) cells, LT-HSCs, short-term HSCs (ST-HSCs) (Lin$^-$cKit$^+$Sca1$^+$CD48$^-$CD150$^-$), or MPPs (Supplemental Figure 4, A–E) between *Edil3*$^{-/-}$ and *Edil3*$^{+/+}$ littermates. Therefore, the observed reduction in myelopoiesis due to Del-1 deficiency could not be attributed to an alteration in absolute cell numbers of hematopoietic progenitor populations in the BM.

Previous studies have shown that FLT3 (Flk2) expression can characterize MPPs with distinct lineage potential (36–38). Analysis of FLT3 expression in MPPs from *Edil3*$^{-/-}$ mice revealed a significant decrease in the percentage of the myeloid-biased FLT3$^-$ MPPs, as compared with *Edil3*$^{+/+}$ mice (Supplemental Figure 4, F and G). Thus, although the total MPP numbers remained unaffected due to Del-1 deficiency, we observed a qualitative difference in MPPs, which displayed a decreased bias toward myeloid differentiation. Consistent with this finding, gene expression analysis demonstrated a significant decrease in the mRNA levels of the myelopoiesis-related genes *Cebpe*, *Csf1r*, *Csf2ra*, and *Irf8* in CD48$^-$LSK cells from *Edil3*$^{-/-}$ mice (Supplemental Figure 4H). Together, these data suggest that Del-1 promotes steady-state myelopoiesis by regulating the bias of early hematopoietic progenitors toward the myeloid lineage.

To assess whether the decreased numbers of myeloid progenitor cells in the BM of *Edil3*$^{-/-}$ mice were due to impaired retention of hematopoietic and myeloid progenitor cells in the BM, we analyzed LSK cells and myeloid progenitor cells in the spleen, as well as circulating LSK cells, myeloid progenitors (LK; Lin$^-$Sca1$^-$cKit$^+$), and CFCs. We did not observe any difference in circulating progenitors (Supplemental Figure 5, A–C), whereas the numbers and frequency of both LSK and LK cells were decreased in the spleen of *Edil3*$^{-/-}$ mice (Supplemental Figure 5, D–G). These data exclude the possibility that the decrease in myeloid progenitor cells in the Del-1–deficient BM was due to enhanced mobilization at steady state and, moreover, suggest a role for Del-1 in promoting HSC differentiation toward the myeloid lineage.

Del-1 promotes the regeneration of myelopoiesis after hematopoietic cell transplantation. We next studied whether Del-1 deficiency

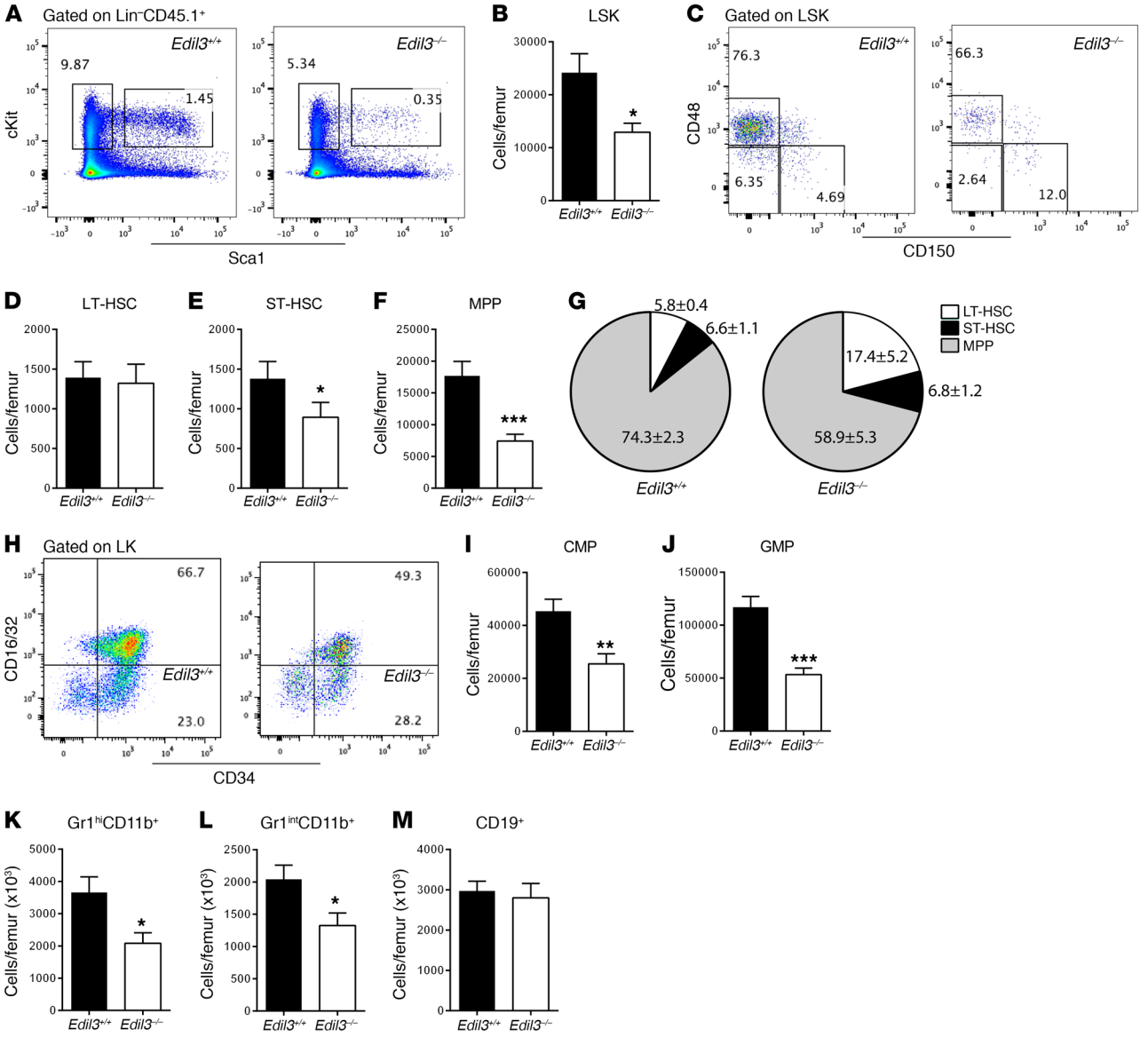

Figure 4. Del-1 in recipient BM promotes the recovery of myelopoiesis. Lethally irradiated *Edil3*$^{+/+}$ or *Edil3*$^{-/-}$ mice (CD45.2) were transplanted with CD45.1$^+$ BM cells, as described in Methods. (**A**) Representative flow cytometry plots and (**B**) number of donor-derived LSK cells (CD45.1$^+$) in the BM of recipient *Edil3*$^{+/+}$ or *Edil3*$^{-/-}$ mice (CD45.2$^+$) at 6 weeks after transplantation (n = 10 mice per group). (**C**) Representative flow cytometry plots and numbers of donor-derived (**D**) LT-HSCs, (**E**) ST-HSCs, and (**F**) MPPs in the BM of recipient *Edil3*$^{+/+}$ or *Edil3*$^{-/-}$ mice at 6 weeks after transplantation (n = 10 mice per group). (**G**) Relative abundance of the indicated cell populations (LT-HSCs, ST-HSCs, and MPPs) in the total LSK population is shown (CD48$^+$CD150$^+$ LSK cells were not considered). (**H**) Representative flow cytometry plots of cells gated on LK (see FACS plot in **A**); (**I**) donor-derived CMP and (**J**) donor-derived GMP cell numbers in the BM of recipient *Edil3*$^{+/+}$ or *Edil3*$^{-/-}$ mice at 6 weeks after transplantation (n = 10 mice per group). Donor-derived (**K**) Gr1^{hi}CD11b$^+$ granulocytes, (**L**) Gr1^{int}CD11b$^+$ myeloid cells, and (**M**) CD19$^+$ B cells in the BM of recipient *Edil3*$^{+/+}$ or *Edil3*$^{-/-}$ mice at 6 weeks after transplantation (n = 10 mice per group). Data are presented as mean ± SEM. Mann-Whitney U test, $^*P < 0.05$, $^{**}P < 0.01$, $^{***}P < 0.001$.

could affect the long-term lineage output of transplanted hematopoietic progenitors. To this end, we generated BM chimeras by transplanting CD45$^+$ BM cells from congenic B6.SJL (CD45.1$^+$) mice into lethally irradiated *Edil3*$^{-/-}$ or *Edil3*$^{+/+}$ mice (CD45.2$^+$) (Figure 3A). At 16 weeks after transplantation, we observed a significant decrease in the percentage of donor-derived Gr1$^+$CD11b$^+$ myeloid cells in the peripheral blood of *Edil3*$^{-/-}$ compared with *Edil3*$^{+/+}$ recipient mice (Figure 3B), with a corresponding increase in the percentage of B cells (Figure 3C). Analysis of BM revealed that this difference was due to impaired reconstitution of myelopoiesis in *Edil3*$^{-/-}$ compared with *Edil3*$^{+/+}$ recipients (Figure 3, D–F), whereas the regeneration of the lymphoid lineage in the BM remained unaffected (Figure 3G). To definitively determine whether Del-1 can affect the long-term lineage bias of transplanted hematopoietic progenitors, we re-transplanted donor-derived cells (CD45.1$^+$) from the *Edil3*$^{+/+}$ recipient mice into secondary *Edil3*$^{+/+}$ and *Edil3*$^{-/-}$ recipients. The observed impairment in myeloid lineage reconstitution in the peripheral blood of secondary *Edil3*$^{-/-}$ recipients was strikingly exacerbated (Figure 3, H and I), indicating that Del-1 in the BM drives the differentiation

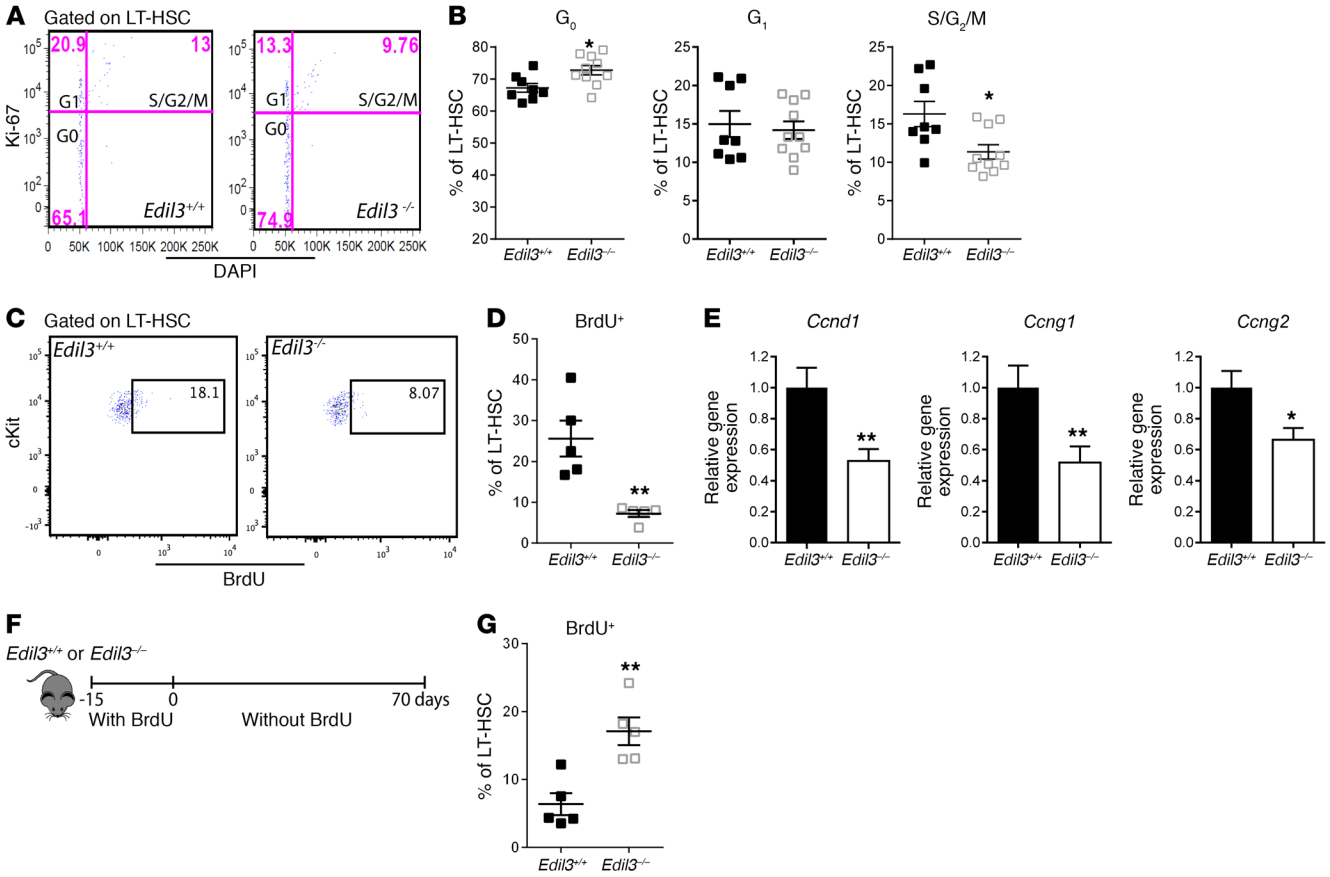

Figure 5. Del-1 promotes LT-HSC cell cycle progression. (**A** and **B**) Staining for Ki-67 nuclear antigen and DNA content (DAPI) was performed for cell cycle analysis. G_0 phase is defined as Ki-67$^-$ and 2n DNA, G_1 as Ki-67$^+$ and 2n DNA, and S-G_2-M as Ki-67$^+$ and DNA >2n. (**A**) Representative flow cytometry plots and (**B**) cell cycle analysis in LT-HSCs from 10-week-old mice (n = 8 *Edil3*$^{+/+}$ and n = 10 *Edil3*$^{-/-}$ mice). K, thousands. (**C**) Representative flow cytometry plots and (**D**) percentage of LT-HSCs that incorporated BrdU after 3 days of BrdU administration in drinking water (n = 5 mice per group). (**E**) Expression of *Ccnd1*, *Ccng1*, and *Ccng2* in LT-HSCs from *Edil3*$^{-/-}$ and *Edil3*$^{+/+}$ mice (n = 11–13 mice per group). mRNA expression was normalized against 18s. (**F**) BrdU pulse-chase assay protocol. BrdU was administered in drinking water for 15 days. Analysis of BrdU-retaining LT-HSCs was performed on day 70 after BrdU withdrawal (n = 5 mice per group). (**G**) Percentage of BrdU-retaining LT-HSCs in the BM of *Edil3*$^{-/-}$ and *Edil3*$^{+/+}$ mice (n = 5 mice per group). Data are presented as mean ± SEM. Mann-Whitney U test, $^*P < 0.05$, $^{**}P < 0.01$.

of hematopoietic progenitors, particularly LT-HSCs, toward the myeloid lineage.

After transplantation, hematopoietic progenitor cells localize in proximity to blood vessels at the endosteal area of the BM (3, 17, 18, 39), which could be attributed to irradiation-induced disruption of sinusoids, though not of endosteal arterioles (3). The expression of Del-1 in the peri-arteriolar region and by OSL cells, which also contribute to the restoration of hematopoiesis after transplantation, prompted us to further investigate in more detail how Del-1 supports the regeneration of myelopoiesis. To this end, we generated BM chimeras by transplanting CD45$^+$ BM cells from congenic B6.SJL (CD45.1$^+$) mice into lethally irradiated *Edil3*$^{-/-}$ or *Edil3*$^{+/+}$ mice (CD45.2$^+$) as above and performed BM analysis at 6 weeks after transplantation. Del-1 deficiency in the BM impaired the expansion of donor-derived hematopoietic cells, as shown by the decreased numbers of donor-derived LSK cells (Figure 4, A and B), ST-HSCs (Figure 4, C and E), and MPPs (Figure 4, C and F), whereas LT-HSC numbers were not altered (Figure 4D). Del-1 deficiency in recipients was associated with an increased percentage of donor-derived LT-HSCs and a concomitant decrease in the percentage of MPPs (Figure 4G), thus pointing to potentially diminished differentiation-associated proliferation of HSCs in the Del-1–deficient recipient environment. These findings were further supported by a decrease in the numbers of myeloid progenitor cells, CMPs and GMPs, in *Edil3*$^{-/-}$ as compared with *Edil3*$^{+/+}$ recipient mice (Figure 4, H–J). These data together suggest that Del-1 promotes the differentiation of hematopoietic progenitor cells into the myeloid lineage after transplantation. Additionally, Del-1 deficiency resulted in reduced numbers of Gr1^{hi}CD11b$^+$ granulocytes (Figure 4K) and Gr1^{int}CD11b$^+$ myeloid cells (Figure 4L), whereas B cell numbers were not affected (Figure 4M). Upon transplantation, therefore, Del-1 promotes hematopoietic progenitor engraftment and differentiation toward the myeloid lineage.

Del-1 deficiency increases LT-HSC quiescence. Since normally there is a strong imbalance in the differentiation output of hematopoietic progenitor cells toward myelopoiesis compared with lymphopoiesis (2, 40), we next investigated whether Del-1 deficiency could affect the proliferation potential of hematopoietic progenitors and thereby the progression of differentiation toward myeloid cell lineage. Cell cycle analysis revealed an increase in LT-HSC

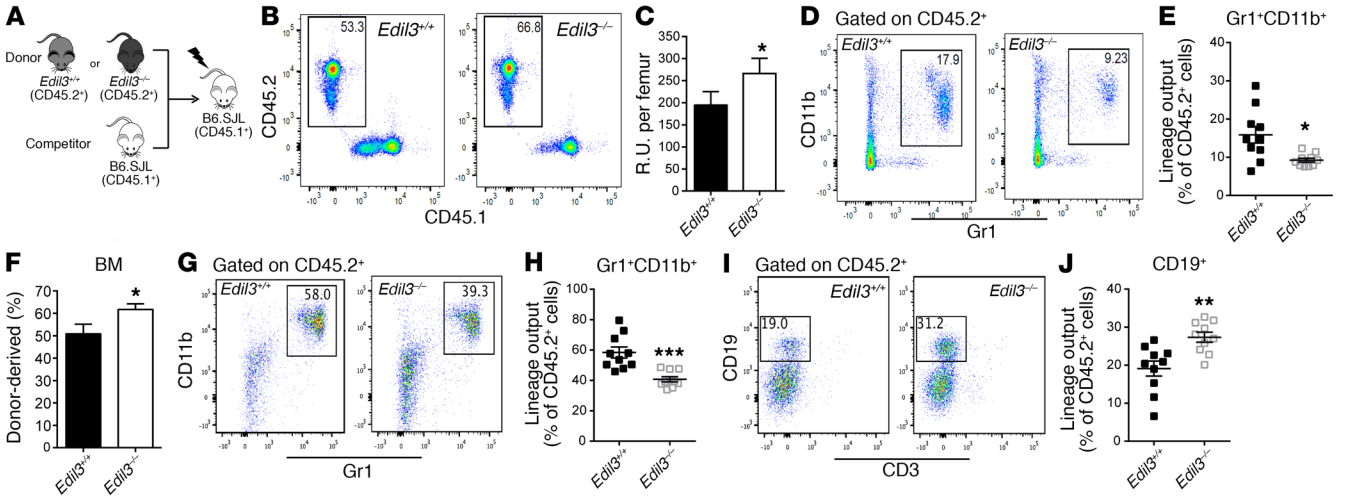

Figure 6. Del-1 deficiency enhances long-term reconstitution capacity and lineage bias of LT-HSCs. (**A**) Competitive repopulation assay: BM cells from either *Edil3*$^{-/-}$ or *Edil3*$^{+/+}$ mice (CD45.2$^+$; donor) and CD45.1$^+$ BM cells as competitors were transplanted into B6.SJL recipient mice (CD45.1$^+$). (**B**) Representative flow cytometry plots of donor-derived chimerism in the peripheral blood of recipient mice at week 16 after transplantation and (**C**) number of R.U. per femur of *Edil3*$^{-/-}$ or *Edil3*$^{+/+}$ donor mice (n = 10 recipients per group). (**D**) Representative flow cytometry plots and (**E**) percentage of donor-derived (CD45.2$^+$) Gr1$^+$CD11b$^+$ myeloid cells in the blood of recipient mice. (**F**) Frequency of donor-derived cells in the BM of recipient mice at 16 weeks after transplantation (n = 10 recipients per group). (**G**) Representative flow cytometry plots and (**H**) percentage of donor-derived (CD45.2$^+$) Gr1$^+$CD11b$^+$ myeloid cells in the BM of recipient mice (n = 10 recipients per group). (**I**) Representative flow cytometry plots and (**J**) percentage of donor-derived CD19$^+$ B cells in the BM of recipient mice at 16 weeks after transplantation (n = 10 recipients per group). Data are presented as mean ± SEM. Mann-Whitney U test, $^*P < 0.05$, $^{**}P < 0.01$, $^{***}P < 0.001$.

quiescence due to Del-1 deficiency, as shown by the increased percentage of LT-HSCs in G_0 phase and the decreased percentage of LT-HSCs in the S/G_2/M fraction in *Edil3*$^{-/-}$ mice (Figure 5, A and B). A BrdU incorporation assay further confirmed the decreased proportion of proliferating LT-HSCs in *Edil3*$^{-/-}$ mice (Figure 5, C and D). The increased quiescence of LT-HSCs from *Edil3*$^{-/-}$ mice compared with LT-HSCs from *Edil3*$^{+/+}$ mice was associated with a downregulation in the gene expression of cyclins *Ccnd1*, *Ccng1*, and *Ccng2* in *Edil3*$^{-/-}$ compared with *Edil3*$^{+/+}$ mice (Figure 5E). Moreover, using a BrdU pulse-chase assay that can identify dormant LT-HSCs (41) (Figure 5F), we found increased frequency of BrdU-retaining (hence dormant) LT-HSCs on day 70 after BrdU withdrawal in *Edil3*$^{-/-}$ as compared with *Edil3*$^{+/+}$ mice (Figure 5G), consistent with the increased quiescence of LT-HSCs in Del-1 deficiency.

Since the engraftment potential of hematopoietic progenitor cells mainly relies on the fraction of cells in the G_0 phase of cell cycle (42, 43), we further assessed whether the enhanced quiescence of LT-HSCs from *Edil3*$^{-/-}$ mice could result in the increased engraftment capacity of these cells. To this end, we performed a competitive transplantation assay by transplanting equal numbers of donor BM cells derived from either *Edil3*$^{-/-}$ or *Edil3*$^{+/+}$ mice (CD45.2$^+$) and competitor cells (CD45.1$^+$) into lethally irradiated recipients (CD45.1$^+$) (Figure 6A). Peripheral blood analysis at 16 weeks after transplantation revealed a significantly increased number of reconstitution units (R.U.) in the BM of *Edil3*$^{-/-}$ donors as compared with their *Edil3*$^{+/+}$ counterparts (Figure 6, B and C). We further assessed the lineage bias of donor cells and observed a decreased frequency of donor-derived (CD45.2$^+$) Gr1$^+$CD11b$^+$ myeloid cells in the blood of recipients transplanted with cells from *Edil3*$^{-/-}$ mice (Figure 6, D and E). Analysis of the BM chimerism in recipient mice further confirmed the increased long-term reconstitution efficiency of progenitors derived from *Edil3*$^{-/-}$ donors (Figure 6F). Additionally, we observed a decreased frequency of Gr1$^+$CD11b$^+$ myeloid cells (Figure 6, G and H) and a corresponding increase in the frequency of CD19$^+$ B cell (Figure 6, I and J) in the donor-derived cell population in the BM of recipients transplanted with cells from *Edil3*$^{-/-}$ mice. Thus, the increased quiescence of LT-HSCs due to Del-1 deficiency results in enhanced repopulation activity of these cells and is associated with decreased myeloid differentiation potential of long-term repopulating cells.

β3 Integrin mediates Del-1–dependent LT-HSC proliferation and myeloid differentiation. Having demonstrated that Del-1 promotes cell cycle progression and myeloid differentiation of hematopoietic progenitors, we set out to address the underlying mechanisms. Through cell-cell and cell-matrix interactions, integrins act as mechanosensors that initiate cell cycle progression via regulation of the levels of cyclins and cyclin-dependent kinase inhibitors (44, 45). In previous studies, we identified the integrins αLβ2 (CD11a/CD18) and αvβ3 (CD51/CD61) as Del-1 receptors (29–31). Therefore, we employed an adhesion assay to determine whether any of these integrins on hematopoietic progenitors mediates interaction with Del-1. Blocking the β3 integrin subunit with anti-CD61 antibody significantly diminished LSK cell adhesion to immobilized Del-1, whereas blockade of CD11a or CD49d had no effect (Figure 7A). We therefore next analyzed CD61 expression on hematopoietic progenitors with flow cytometry and found that CD61 was highly expressed on LT-HSCs and to a lesser extent on MPPs (Figure 7, B and C), which is in accordance with earlier studies (46, 47). To test the hypothesis that the interaction of Del-1 with the αvβ3 integrin on hematopoietic progenitors regulates cell cycle–related gene expression, we cultured isolated LSK cells on immobilized Del-1 expressed as an Fc fusion protein (Del-1–Fc) or Del-1[RGE]–Fc, a point mutant that precludes interaction with αvβ3 integrin due to a Glu (E) for Asp (D) substitution in the critical

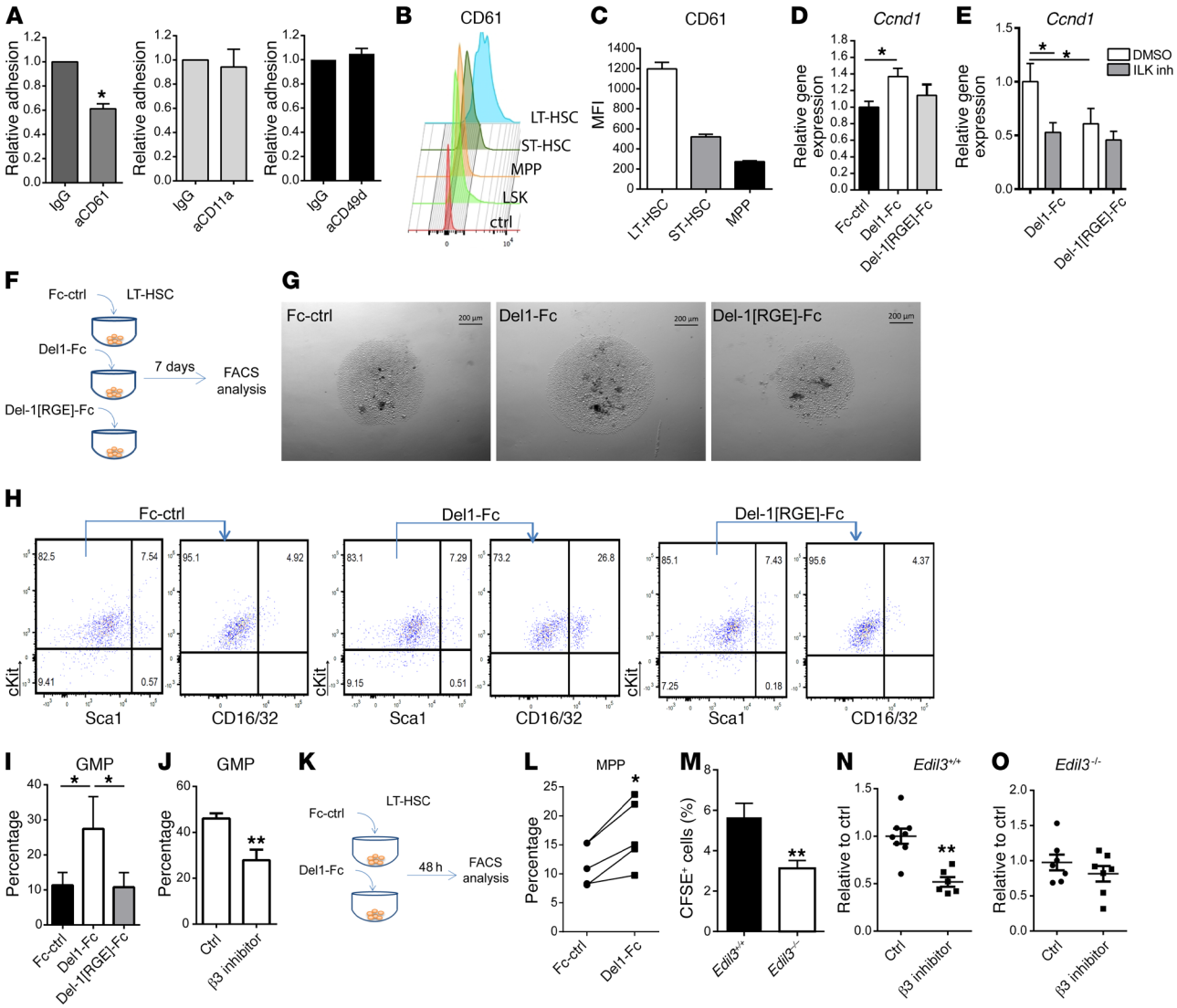

Figure 7. αvβ3 mediates the interaction of hematopoietic progenitors with Del-1. (**A**) Inhibition of LSK cell adhesion onto immobilized Del-1 by anti-CD61 (anti-β3) but not by anti-CD11a antibody or anti-CD49d antibody using a static adhesion assay (n = 3–4 independent experiments). Appropriate isotype control antibodies were used; cell adhesion in the presence of isotype controls was set as 1. (**B** and **C**) Expression of CD61 (β3 integrin) on hematopoietic progenitor cells was studied by flow cytometry. (**B**) Representative histograms and (**C**) median fluorescent intensity (MFI) are shown (n = 5). (**D**) *Ccnd1* expression in LSK cells cultured for 3 hours on Fc-control protein, Del-1–Fc, or Del-1-Fc mutated in the RGD motif (Del-1[RGE]–Fc) (n = 5 independent experiments). *Ccnd1* expression in LSK cells is shown relative to control (Fc-control protein [Fc-ctrl]). (**E**) Effect of ILK inhibition [ILK inh] in Del-1–dependent upregulation of *Ccnd1* expression (n = 4 independent experiments). DMSO was used as control. *Ccnd1* expression in LSK cells is shown relative to Del-1–Fc in the presence of DMSO. (**F**) Experimental design for the differentiation assay. LT-HSCs from mice were cultured with Del-1–Fc or Fc-control or Del-1[RGE]–Fc (500 ng/ml each) in cell suspension cultures, and analysis was performed after 7 days. (**G**) Representative images of the colonies, (**H**) representative flow cytometry plots, and (**I**) percentage of GMPs (n = 4 cultures). Scale bars: 200 μm. (**J**) LT-HSCs were cultured with Del-1–Fc in the presence of a β3 inhibitor or control peptide (25 μg/ml each) for 7 days, as described in **F**, and the percentage of GMPs was assessed by flow cytometry (n = 5 cultures). (**K**) Experimental design for the differentiation assay. LT-HSCs were cultured with Del-1-Fc or Fc-control (500 ng/ml each) for 48 hours, and (**L**) the percentage of MPPs was analyzed by flow cytometry (n = 5 cultures). (**M**) Accumulation of CFSE$^+$ LSK cells in the BM of non-irradiated recipient *Edil3*$^{-/-}$ (n = 9) or *Edil3*$^{+/+}$ mice (n = 11) 20 hours after adoptive transfer of CFSE-labeled Lin$^-$ cells from WT mice. Cell accumulation in the BM is expressed as the percentage of CFSE$^+$ LSK in total LSK cells. (**N**) Accumulation of CFSE$^+$ LSK cells in the BM of non-irradiated recipient *Edil3*$^{+/+}$ mice at 20 hours after adoptive transfer of CFSE-labeled Lin$^-$ cells from WT mice pretreated with a β3 inhibitor (n = 6) or control peptide (n = 8 mice), as described in Methods. (**O**) Accumulation of CFSE$^+$ LSK cells in the BM of non-irradiated recipient *Edil3*$^{-/-}$ mice at 20 hours after adoptive transfer of CFSE-labeled Lin$^-$ cells from WT mice pretreated with a β3 inhibitor or control peptide (n = 7 mice per group). Cell accumulation in the BM is shown as relative to control peptide (ctrl) in **N** and **O**. Data are presented as mean ± SEM. Student's paired t test was used in **A**, **J**, and **L**. One-way ANOVA followed by Holm-Šidák's multiple comparison test was used in **D**, **E**, and **I**. Mann-Whitney U test was used in **M**–**O**. *$P < 0.05$, **$P < 0.01$.

RGD motif. Fc protein was used as a negative control. In contrast to the WT molecule, the RGE point mutant failed to induce *Ccnd1* gene expression in LSK cells (Figure 7, D and E), thus indicating a requirement for αvβ3-dependent adhesion to Del-1 for induction of *Ccnd1*. To independently confirm that signaling induced through Del-1 ligation of αvβ3 integrin was responsible for regulating cyclin D1 expression, we used an inhibitor of integrin-linked kinase (ILK), which mediates integrin-dependent outside-in sig-

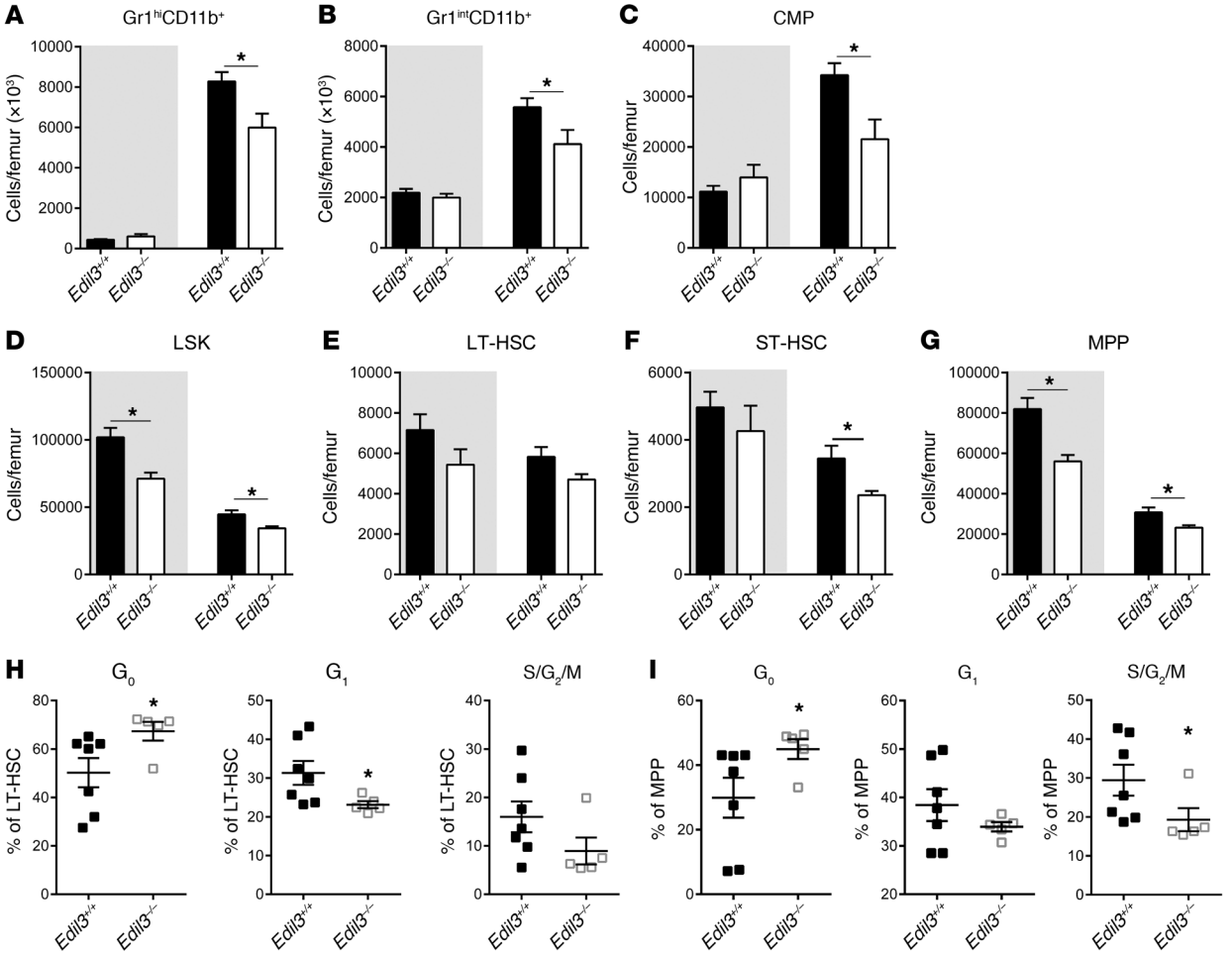

Figure 8. Del-1 mediates the restoration of myelopoiesis in the BM upon LPS-induced inflammation. (**A**) Gr1^{hi}CD11b^{+} granulocytes and (**B**) Gr1^{int}CD11b^{+} myeloid cell numbers in the BM of *Edil3*$^{+/+}$ or *Edil3*$^{-/-}$ mice at 24 hours (gray background) and at 72 hours following the second injection of LPS (n = 4–10 mice per group). (**C**) CMP, (**D**) LSK, (**E**) LT-HSC, (**F**) ST-HSC, and (**G**) MPP cell numbers in the BM of *Edil3*$^{-/-}$ and *Edil3*$^{+/+}$ mice (n = 4–8 mice per group) at 24 hours (gray background) and at 72 hours following the second injection of LPS. (**H**) Cell cycle analysis in LT-HSCs and (**I**) MPPs at 72 hours following the second injection of LPS (n = 5–7 mice per group). Data presented as mean ± SEM. Mann-Whitney U test. *$P < 0.05$.

naling. We found that ILK inhibition abrogated the effect of the αvβ3–Del-1 interaction on *Ccnd1* expression (Figure 7E). These findings reveal a role for Del-1 in regulating cyclin D1 expression in progenitors via interaction with αvβ3 integrin and integrin-dependent outside-in signaling events.

To further study whether Del-1 can drive the proliferation and differentiation of early progenitor cells, we performed an in vitro differentiation assay. LT-HSCs were treated with Fc-control, Del-1–Fc, or Del-1[RGE]–Fc in cell suspension cultures (Figure 7F). Del-1–Fc (but not Fc-control) induced the proliferation and differentiation of LT-HSCs toward GMPs, whereas this effect was abolished when the RGE point mutant was used (Figure 7, G–I). Inhibition of β3 integrins by a β3 inhibitor, cilengitide, also abrogated LT-HSC differentiation on day 7 (Figure 7J), further suggesting the involvement of β3 integrins in Del-1–dependent induction of LT-HSC differentiation. To further determine whether Del-1 acts on LT-HSCs or at later stages of differentiation, we treated LT-HSCs, MPPs, or CMPs for 48 hours with Fc-control or Del-1–Fc (Figure 7K and Supplemental Figure 6). We observed that Del-1 induced the differentiation toward MPPs (Figure 7L), whereas it had no effect on the differentiation of MPPs or CMPs toward GMPs (Supplemental Figure 6). These experiments firmly establish that the direct interaction of LT-HSC with Del-1 instructs their differentiation toward the myeloid lineage.

We next addressed the in vivo relevance of the Del-1/β3 integrin interaction. To this end, we initially studied the role of Del-1 in hematopoietic progenitor cell homing to the BM. Fluorescently labeled Lin^{-} cells were transplanted to non-ablated *Edil3*$^{-/-}$ and *Edil3*$^{+/+}$ mice, and the percentage of transferred LSK cells in the BM was assessed 3 or 20 hours later. Del-1 deficiency had no effect at the early time point (Supplemental Figure 7). Therefore, Del-1 does not affect the initial recruitment of hematopoietic progenitors via the vasculature to the BM, consistent with the fact that Del-1 does not interact with or regulate the α4β1 integrin (29) (Figure 7A), which is required for this function (48). Intriguingly, at the 20-hour time point, the percentage of transferred cells was significantly decreased in *Edil3*$^{-/-}$ as compared with *Edil3*$^{+/+}$ mice, hence implicating Del-1 in the homing of transplanted hematopoietic progenitors (Figure 7M). To assess the significance of β3 integrin–dependent interactions of Del-1 in the BM, we tested whether this

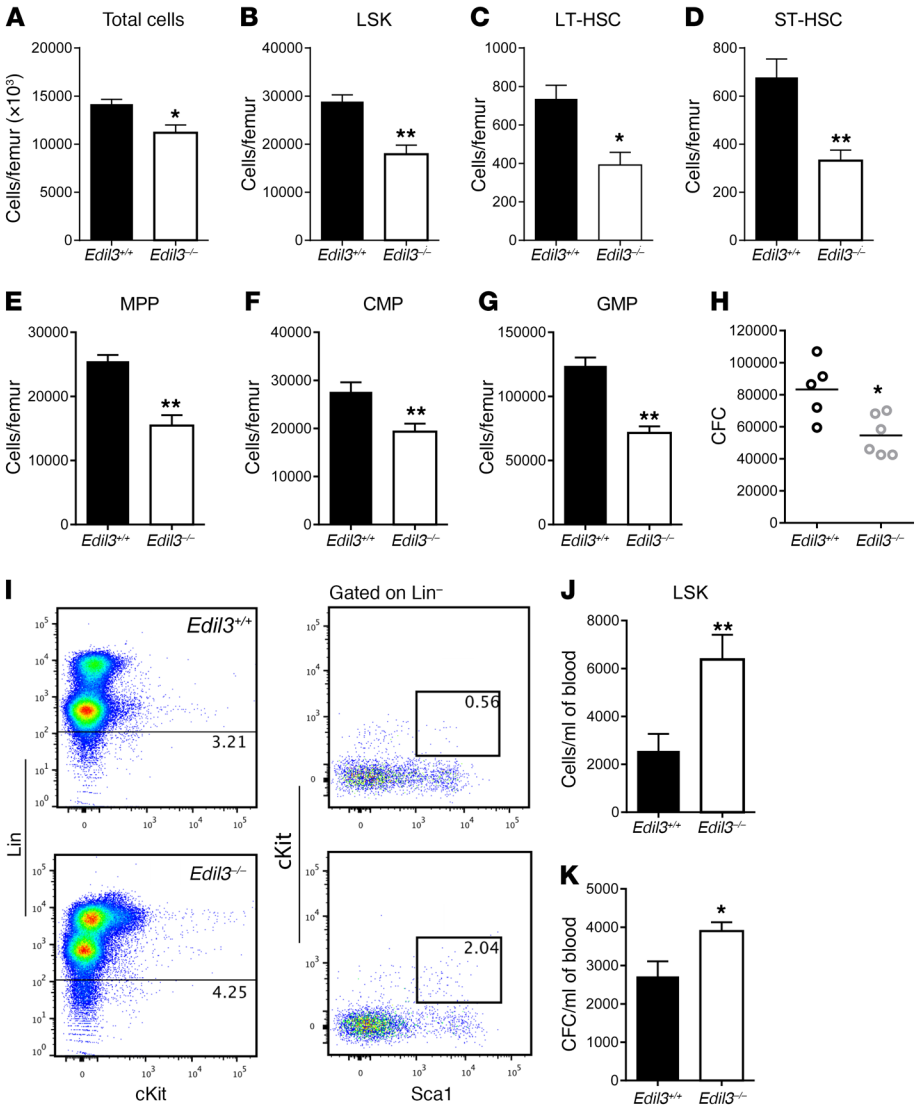

Figure 9. Role of Del-1 in the response of hematopoietic progenitor cells to G-CSF administration. (**A**) Total cell numbers and (**B**) LSK, (**C**) LT-HSC, (**D**) ST-HSC, (**E**) MPP, (**F**) CMP, and (**G**) GMP cell numbers in the BM of *Edil3*$^{-/-}$ and *Edil3*$^{+/+}$ mice (n = 6 per group) at the end of the G-CSF administration protocol. (**H**) CFCs from the BM of *Edil3*$^{-/-}$ (n = 6) and *Edil3*$^{+/+}$ mice (n = 5) at the end of the G-CSF administration protocol. (**I**) Representative flow cytometry plots and (**J**) numbers of mobilized LSK cells in the peripheral blood of *Edil3*$^{-/-}$ (n = 10) and *Edil3*$^{+/+}$ mice (n = 11) at the end of the G-CSF administration protocol. (**K**) Number of CFCs in the peripheral blood of *Edil3*$^{-/-}$ and *Edil3*$^{+/+}$ mice (n = 5-6 mice) at the end of the G-CSF administration protocol. Data are presented as mean ± SEM. Mann-Whitney U test, $^{*}P < 0.05$, $^{**}P < 0.01$.

integrin mediates the enhanced homing of hematopoietic progenitors to the Del-1–proficient BM relative to the Del-1–deficient BM environment. To this end, fluorescently labeled Lin^{-} cells from WT mice were transplanted to *Edil3*$^{-/-}$ or *Edil3*$^{+/+}$ littermates, together with a β3 inhibitor (cilengitide) or control peptide. Upon transplantation into *Edil3*$^{+/+}$ mouse recipients, inhibition of β3 integrin decreased the homing of LSK cells to the BM, as compared with control treatment (Figure 7N). In contrast, β3 inhibition did not affect the homing of LSK to the BM of *Edil3*$^{-/-}$ recipients (Figure 7O), suggesting that β3 integrin and Del-1 lie in the same pathway and contribute to the same homing mechanism for hematopoietic progenitors to the BM.

Integrin αvβ3 has been previously shown to mediate the maintenance of HSCs, although the natural ligand(s) required for this niche interaction were not identified (46, 47). Having shown that the Del-1/β3 integrin interaction plays a role in the homing of hematopoietic progenitors into the BM, we then determined whether this interaction also contributes to the restoration of myelopoiesis after transplantation. For this purpose, CD45^{+} BM cells from *Itgb3*$^{-/-}$ mice were transferred into lethally irradiated *Edil3*$^{-/-}$ or *Edil3*$^{+/+}$ mice, and BM analysis in the recipient mice was performed 6 weeks later (Supplemental Figure 8A). As this experiment was not done using the congenic CD45.1/CD45.2 system, it was not possible to specifically study the reconstitution by donor-derived cells. For this reason, analysis was performed by determining the absolute cell numbers of different hematopoietic progenitor populations in the BM of recipient mice. Consistent with the above-described effects of β3 integrin inhibition, in the absence of β3 integrin on donor cells, Del-1 deficiency in recipients failed to affect the number of LSK cells, myeloid progenitors, or Gr1^{hi}CD11b^{+} granulocytes and Gr1^{int}CD11b^{+} myeloid cell populations (Supplemental Figure 8, B–F). These findings stand in stark contrast to the negative effect of Del-1 deficiency on myelopoiesis reconstitution upon transplantation of β3 integrin–sufficient donor cells (Figure 4). Therefore, β3 integrin is required for the Del-1–mediated progenitor engraftment and reconstitution of myelopoiesis after transplantation.

Del-1 promotes the response of hematopoietic progenitors to systemic inflammation. The above-documented function of Del-1 in steady-state myelopoiesis and in the regeneration of the myeloid lineage after transplantation prompted us to investigate its possible involvement in the response of hematopoietic progenitors to stress granulopoiesis, such as in models induced by LPS or G-CSF.

Administration of high-dose LPS is widely used to mimic the effect of systemic microbial infection on granulopoiesis, which forces LSK proliferation to compensate for the increased need for mature myeloid cells and restore BM cellularity (49–51). We therefore engaged this model to investigate whether Del-1 in the niche regulates the potential for myeloid lineage replenishment in the BM. To this end, *Edil3*$^{-/-}$ or *Edil3*$^{+/+}$ mice were intraperito-

neally injected with ultra-pure LPS twice, with an interval of 48 hours, and hematopoietic progenitors and myeloid lineage cells were analyzed at 24 hours and at 72 hours following the second injection (52, 53). In this model, the initial increase in peripheral blood myeloid cells (52, 53), associated with a decrease in the numbers of mature myeloid cells and CMPs in the BM, is followed by a prominent expansion of the myeloid cell compartment, as observed in *Edil3*$^{+/+}$ mice at 72 hours after LPS administration (Figure 8, A and B). However, the restoration of myelopoiesis in the BM was significantly attenuated in Del-1 deficiency, as shown by the decreased numbers of Gr1^{hi}CD11b^{+} granulocytes (Figure 8A) and Gr1^{int}CD11b^{+} myeloid cells (Figure 8B) in *Edil3*$^{-/-}$ relative to *Edil3*$^{+/+}$ mice. In the same vein, the numbers of CMPs were decreased in *Edil3*$^{-/-}$ compared with *Edil3*$^{+/+}$ mice at 72 hours after LPS administration (Figure 8C). Furthermore, Del-1 deficiency resulted in relatively inefficient expansion of LSK cells caused predominantly by inefficient expansion of MPPs 24 hours after LPS injection, and these differences between *Edil3*$^{-/-}$ and *Edil3*$^{+/+}$ mice were sustained after 72 hours (Figure 8, D–G). The delay in the reconstitution of the myeloid lineage was also associated with an increase in the percentage of quiescent LT-HSCs and MPPs (Figure 8, H and I) after 72 hours. In contrast, no difference was observed in cell cycle progression of myeloid progenitor cells upon LPS injection due to Del-1 deficiency (data not shown). No alterations in G-CSF production, which plays a critical role in emergency granulopoiesis (54), were observed between *Edil3*$^{-/-}$ and *Edil3*$^{+/+}$ mice (Supplemental Figure 9). In addition, the expression of *Edil3* in the BM was not altered after LPS administration (data not shown). Furthermore, we did not observe any difference in the number of LSK and LK cells in the peripheral blood or spleen between Del-1–deficient and –proficient mice (Supplemental Figure 10). The data in toto demonstrate that Del-1 promotes myeloid cell replenishment in the BM in the course of systemic inflammation.

Del-1 regulates hematopoietic progenitor proliferation and retention in response to G-CSF. Besides inducing myeloid progenitor maturation (54), G-CSF was previously shown to promote LSK cell expansion by affecting the LT-HSC cell cycle (55, 56). For this reason, adult *Edil3*$^{-/-}$ and *Edil3*$^{+/+}$ mice were injected daily with G-CSF for up to 6 days. At 24 hours after a single G-CSF administration, the expansion of total BM cells (Supplemental Figure 11A), Gr1^{hi}CD11b^{+} granulocytes (Supplemental Figure 11B), and Gr1^{int}CD11b^{+} myeloid cells (Supplemental Figure 11C) was less prominent in *Edil3*$^{-/-}$ than in *Edil3*$^{+/+}$ mice. LSK cell, MPP, and CMP but not LT-HSC or ST-HSC numbers (Supplemental Figure 11, D–H) were also decreased in *Edil3*$^{-/-}$ relative to *Edil3*$^{+/+}$ mice. Cell cycle analysis of LT-HSCs from *Edil3*$^{-/-}$ and *Edil3*$^{+/+}$ mice after 3 daily injections of G-CSF revealed a decrease in the proliferation potential in HSCs derived from *Edil3*$^{-/-}$ mice (Supplemental Figure 11, I and J). By the end of the G-CSF administration course (6 days), BM cellularity (Figure 9A) and numbers of hematopoietic and myeloid progenitors (Figure 9, B–G) were dramatically reduced in *Edil3*$^{-/-}$ mice as compared with *Edil3*$^{+/+}$ mice. The decrease in phenotypical progenitor cells in Del-1 deficiency by the end of the G-CSF administration course was also associated with reduced counts of functional progenitor cells, as shown by a CFU assay (Figure 9H). To further evaluate whether Del-1 deficiency affects myelopoiesis upon G-CSF administration, the percentage of GMPs and LSK cells in the BM after 6 daily injections of G-CSF was expressed relative to the percentage of GMPs and LSK cells in the BM after 6 daily injections of PBS. The corresponding ratios were then compared between *Edil3*$^{-/-}$ and *Edil3*$^{+/+}$ mice. We observed that the expansion of GMPs in the BM of *Edil3*$^{+/+}$ mice was more robust compared with *Edil3*$^{-/-}$ mice (Supplemental Figure 12A). Additionally, the relative levels of LSK cells were also significantly higher in *Edil3*$^{+/+}$ mice (Supplemental Figure 12B).

As G-CSF is used as a mobilizing agent in the context of autologous or allogeneic transplant (21, 23), we examined whether the physical interaction between Del-1 and HSCs promotes their retention in the BM, thereby counteracting the mobilizing effect of G-CSF. G-CSF–dependent mobilization of hematopoietic progenitor cells was more efficient in Del-1 deficiency, as shown by the increased numbers of LSK (Figure 9, I and J) and CFCs (Figure 9K) in the peripheral blood of *Edil3*$^{-/-}$ mice. We did not observe any alterations in the expression of *Edil3* in the endosteal region of mice by the end of the G-CSF administration protocol (data not shown). Since downregulation in the expression of HSC niche factors in MSCs and osteoblasts is an important event during G-CSF–dependent mobilization (12, 57, 58), we assessed *Cxcl12*, *Angpt1*, and *Kitl* gene expression in the endosteal region of *Edil3*$^{-/-}$ and *Edil3*$^{+/+}$ mice after 6 daily injections of G-CSF. We observed that the decrease in the mRNA levels of these factors followed the same pattern in *Edil3*$^{+/+}$ and *Edil3*$^{-/-}$ mice (Supplemental Figure 13). Therefore, the effect of Del-1 deficiency on G-CSF–induced mobilization cannot be attributed to alterations in the expression of other HSC niche factors. These findings overall indicate that Del-1 acts as a niche factor that supports hematopoietic progenitor retention in the BM upon G-CSF–induced mobilization.

Discussion

Herein, we detected that Del-1 was enriched in the perivascular area of the BM, expressed by critical cellular niche components. Moreover, Del-1, via its interaction with β3 integrin on LT-HSCs, facilitated LT-HSC proliferation and differentiation toward the myeloid lineage under steady-state and hematopoietic stress conditions. Our data therefore establish a role for Del-1 in the HSC niche microenvironment.

During steady-state hematopoiesis, Del-1 deficiency resulted in increased quiescence of LT-HSCs without affecting hematopoietic progenitor cell numbers, which is in accordance with previous studies showing that deficiency of niche factors does not necessarily have a quantitative effect on LT-HSCs (5, 59). Strikingly, however, Del-1 deficiency resulted in a significant decrease in myeloid cell populations. Steady-state myelopoiesis is mainly maintained by multipotent hematopoietic progenitor cells (2). Consistent with this finding, we detected a significant downregulation in the expression levels of myelopoiesis-related genes in CD48^{-} LSK cells derived from Del-1–deficient mice. Moreover, Del-1 deficiency resulted in phenotypic changes in MPPs, leading to a decreased percentage of MPPs with low Flt3 expression, which have been previously shown to be biased toward differentiation into myeloid lineage (36–38). Del-1 deficiency was further shown to affect the lineage bias of LT-HSCs, as shown by competitive repopulation conditions. The enhanced engraftment potential of hematopoietic progenitors from *Edil3*$^{-/-}$ mice was linked to a diminished poten-

tial for production of myeloid cells, which is in line with recent studies showing an association between increased proliferation of LT-HSCs and myeloid differentiation bias (60, 61). In particular, HSC clones with high proliferation rates were recently shown to be biased toward myeloid differentiation, while another study revealed a correlation between the expression of cell cycle and DNA replication genes and that of myeloid differentiation genes (60, 61). Our findings that Del-1 regulated the proliferation potential and myeloid differentiation of LT-HSCs but not of MPPs or CMPs suggest that Del-1 likely promotes differentiation-associated proliferation of LT-HSCs, thereby enabling the response of hematopoiesis to increased needs for production of myeloid cells.

The effect of Del-1 deficiency on LT-HSC proliferation potential and myelopoiesis had a strong impact in distinct models of stress myelopoiesis, wherein induction of hematopoietic progenitor proliferation is required to effectively replenish BM cells (1, 40). Using three different, clinically relevant models, we demonstrated that Del-1 is essential for the proper hematopoietic progenitor response with regard to myeloid cell reconstitution, after BM transplantation, G-CSF administration, and LPS-dependent inflammation. In all three models, Del-1 deficiency consistently compromised the ability of the niche microenvironment to support the proliferation and differentiation of LT-HSCs into the myeloid lineage. After hematopoietic cell transplantation, Del-1 in the recipient niche promoted progenitor engraftment and the generation of both progenitors and mature cells of the myeloid lineage in a manner dependent upon β3 integrin expression in hematopoietic cells. Similarly, Del-1 was found to contribute to the proliferative response of hematopoietic progenitor cells after G-CSF administration or LPS-driven inflammation. Moreover, Del-1 promoted the retention of hematopoietic progenitors in the BM upon G-CSF administration. The critical involvement of Del-1 in all these different models of stress myelopoiesis attests to the important regulatory role of Del-1 within the HSC niche for myeloid lineage commitment.

The αvβ3 integrin on LT-HSCs interacted with and mediated the Del-1–dependent progenitor retention in the BM and progenitor commitment toward the myeloid lineage. The αvβ3 integrin/Del-1 interaction supported LT-HSC differentiation–associated proliferation, which involved the induction of cyclin D1 expression. Previous studies have shown that αvβ3 integrin is expressed in HSCs and supports the maintenance of HSC activity (46, 47), although the niche-relevant ligand(s) of αvβ3 were not determined. Integrin activation is tightly linked to cell survival and proliferation (45). Cell-cell or cell–extracellular matrix adhesion through integrins induces intracellular signaling pathways that enable cells to enter cell cycle (45). The expression of D-cyclins is controlled by the extracellular environment (62) and is essential for integrin-mediated progression through the G_1 phase of the cycle (44, 63). The important role of cyclin D1 in LT-HSC function was further highlighted in a recent study where downregulation of cyclin D1 gene expression, due to alterations in cell metabolism, exerted a critical impact on normal and leukemic HSC function (64). Additionally, cyclin D1 expression has been previously associated with HSC differentiation–associated proliferation (42). We demonstrate here that the decreased proliferation of LT-HSCs due to Del-1 deficiency in vivo is associated with reduced mRNA levels of *Ccnd1*, whereas the interaction between Del-1 and αvβ3 integrin on hematopoietic progenitors results in increased *Ccnd1* expression. The Del-1 deficiency–associated decreased gene expression of *Ccnd1* in hematopoietic progenitors together with the in vitro stimulatory effect of Del-1 on *Ccnd1* expression strongly corroborates the evidence presented here that Del-1 acts as a niche factor mediating differentiation-associated proliferation and myeloid lineage commitment of HSCs.

Several cellular components have been implicated as contributing to homeostatic HSC niche function. Arteriolar vessels, comprising endothelial cells and a layer of mesenchymal stromal cells, promote the maintenance of LT-HSCs in a quiescent state (6, 7, 13), although non-dividing stem cells have also been localized around sinusoids (6, 10). Endothelial and perivascular stromal cells, including CAR cells, support the maintenance of HSCs in the niche by producing stem cell factor, pleiotrophin, and CXCL12 (6, 7, 9, 11–16) or by direct adhesive interactions through molecules, such as E-selectin (5). While expression of E-selectin is restricted to the endothelium, thus representing an endothelial-specific niche, Del-1 is expressed by several major cellular components in the niche microenvironment (CAR, arteriolar endothelial, and OSL cells). Therefore, Del-1 can act as a crucial HSC niche regulator in different settings. Indeed, by multiple complementary experimental approaches, we have demonstrated that Del-1 promotes the retention of hematopoietic progenitors in the niche and orchestrates their proliferation and differentiation into the myeloid lineage under diverse conditions, ranging from steady-state to regenerative and inflammation-related myelopoiesis. Thus, the demonstration of Del-1 as a factor governing the proliferation and fate of LT-HSC provides mechanistic insights into how the HSC niche operates and contributes to homeostatic adaptation of the hematopoietic system. Interestingly, the adhesive interaction between niche-expressed Del-1 and the αvβ3 integrin on LT-HSCs also constitutes an example of juxtacrine regulation of progenitor commitment toward the myeloid lineage. Our findings thereby identify what we believe to be a novel spatial component in the regulation of lineage fate and add to the growing evidence of distinct control of hematopoietic precursors within the BM.

Our findings establish a homeostatic role for Del-1 during inflammation via stimulation of myelopoiesis and production of mature effector cells. Therefore, the homeostatic function of Del-1 is not restricted to regulation of inflammatory cell recruitment to peripheral tissues as we showed earlier (29, 31, 65), but also involves control of their progenitors in the BM. As febrile neutropenia, associated with chemotherapy or HSC transplantation, is a major cause for morbidity and mortality (25), the herein identified role of Del-1 in the induction and maintenance of proper de novo granulopoiesis is important and could be therapeutically exploited in this context. On the other hand, inhibition of the interaction of Del-1 with hematopoietic progenitor cells could be exploited pharmacologically to enhance progenitor mobilization in the context of autologous or allogeneic HSC transplantation or hematologic malignancy (66). The emergence of Del-1 as a critical niche factor that promotes hematopoietic progenitor expansion and retention, as well as myelopoiesis, suggests that this homeostatic factor needs to be seriously considered in the context of BM transplantation or hematological disorders.

Methods

Animals and transplantation experiments. *Edil3*$^{-/-}$ mice in a C57BL/6 background were previously described (29, 31). CXCL12-GFP mice were housed in a specific pathogen–free facility at Fundación CNIC and were previously described (33, 34). Mice deficient in β3 integrin (*B6;129S2-Itgb3*^{tm1Hyn}/J; stock no. 004669) and C57BL/6-CD45.1 B6.SJL-*Ptprca Pepcb*/BoyJ (B6/SJL) mice were from the Jackson Laboratory. Sex- and age-matched mice were used.

To generate BM chimeras, a total of 2×10^6 CD45$^+$ BM cells from B6/SJL (CD45.1) mice were retro-orbitally transplanted into lethally irradiated (9 Gy) *Edil3*$^{-/-}$ or *Edil3*$^{+/+}$ (WT) littermate mice (CD45.2). Blood was collected at week 16 for analysis of donor-derived peripheral blood cells, and BM analysis was performed at 6 and 16 weeks after transplantation for the analysis of donor-derived (CD45.1) cell populations. At week 16 after transplantation, a total of 2×10^6 CD45.1$^+$ BM cells from the *Edil3*$^{+/+}$ recipient group were further transplanted into lethally irradiated (9 Gy) *Edil3*$^{-/-}$ or *Edil3*$^{+/+}$ mice (CD45.2), and peripheral blood analysis of the frequency of different CD45.1$^+$ cell populations was performed every 4 weeks. In additional experiments, 2×10^6 CD45$^+$ BM cells from *Itgb3*$^{-/-}$ mice (CD45.2) were retro-orbitally transplanted into lethally irradiated *Edil3*$^{-/-}$ or *Edil3*$^{+/+}$ mice. The reconstitution of different cell populations in the BM of the recipient mice was analyzed at week 6 after transplantation.

For BM competitive repopulation assays, the CD45.1/CD45.2 congenic system was used. Equivalent volumes of BM cells (2.5% of cells derived from a femur) harvested from CD45.2$^+$ donor mice (*Edil3*$^{-/-}$ and *Edil3*$^{+/-}$) were retro-orbitally transplanted into lethally irradiated B6/SJL (CD45.1) recipients along with 3×10^5 BM cells derived from B6/SJL mice (67). Peripheral blood chimerism was assessed at 16 weeks after transplantation. We calculated the number of injected R.U. per recipient mouse using the formula $(D \times C)/(100 - D)$, where D is the percentage of CD45.2$^+$ blood leukocytes at 16 weeks in the recipient mice, and C is the number of competing CD45.1$^+$ R.U. that were coinjected ($C = 3$, since 3×10^5 competing BM cells were injected). The number of R.U. per femur was calculated afterward (5, 68). Chimerism in BM cells was also analyzed at week 16. Analysis of the lineage output of donor-derived (CD45.2$^+$) cells was further performed after gating on donor-derived cells. In all transplantation experiments, mice were kept on antibiotic-containing water for 2 weeks after irradiation.

To assess the effect of Del-1 in hematopoietic progenitor migration to and homing in the BM, 2×10^6 Lin$^-$ cells from *Edil3*$^{+/+}$ mice were labeled with CFSE and were retro-orbitally transferred into non-irradiated *Edil3*$^{-/-}$ or *Edil3*$^{+/+}$ littermate recipients. BM was analyzed 3 or 20 hours after cell transfer. In other experiments, CFSE$^+$ Lin$^-$ cells from *Edil3*$^{+/+}$ mice were pretreated for 5 minutes with cilengitide (10 mg/kg; Selleck Chemicals) (69) or RGD control peptide (10 mg/kg; Enzo Life Sciences, GRADSP) before their transfer into non-irradiated *Edil3*$^{-/-}$ or *Edil3*$^{+/+}$ littermate recipients.

Primary human cells. Primary human MSCs from healthy donors were generated out of BM aspirates by applying plastic adherence and serial passaging, as previously described (70–74). MSCs of the second passage were cultured in 24-well culture plates in DMEM supplemented with 10% FBS until reaching subconfluence, then the medium was changed to DMEM with 0.1% BSA (Sigma-Aldrich); supernatants were collected 18 and 48 hours thereafter. HUVECs (Lonza) were cultured in complete EBM-2 medium (Lonza). Cell pellets from human osteoblasts were from PromoCell. Total RNA was extracted using TRI reagent (Molecular Research Center Inc.). Del-1 concentration in culture supernatants was measured using a human EDIL3 DuoSet ELISA (R&D Systems).

BrdU incorporation and pulse-chase assay. For BrdU incorporation assay, BrdU was administered in drinking water for 3 days at a concentration of 0.5 mg/ml (5). For BrdU pulse-chase assay, BrdU was administered in drinking water for 15 days at a concentration of 0.5 mg/ml. Drinking water was changed twice weekly. Water containing BrdU was replaced with regular water after the pulse period, and analysis was performed 70 days after BrdU withdrawal (41). Staining for BrdU was performed using the FITC BrdU Flow Kit (BD Biosciences) following the manufacturer's instructions.

LPS and G-CSF administration. To assess the effect of G-CSF on hematopoietic progenitors, we injected mice subcutaneously with a daily dose of 250 μg/kg of recombinant human G-CSF (Amgen) in PBS (Life Technologies) or PBS as control for up to 6 days. For LPS-induced inflammation, mice were injected intraperitoneally with 35 μg ultrapure LPS (*E. coli* 0111:B4; InvivoGen) twice, with a 48-hour interval, and sacrificed at 24 hours or at 72 hours following the second injection. In the LPS model, only BM samples with viability >80 % were included in analysis. Peripheral blood analysis was performed using a Sysmex XT-2000 blood analyzer (Sysmex Corp.).

Flow cytometry, sorting, and immunofluorescence. Cell analysis was performed with a FACSCanto II flow cytometer using FACSDiva 6.1.3 software (BD) or FACS LSR II flow cytometer. BM cells were harvested from femurs by repeatedly flushing with PBS supplemented with 5% FBS (Life Technologies). Mouse spleens were homogenized, and single-cell suspensions were prepared after erythrocyte lysis with red blood cell lysis buffer (eBioscience). The analysis of BM and spleen cellularity was performed with MACSQuant (Miltenyi Biotec). The antibodies used for cell surface phenotype analysis are shown in Supplemental Table 1. Brilliant Violet 510 Streptavidin (BioLegend) was used for the detection of biotinylated antibodies. Cell viability was assessed using Hoechst 33258 (Life Technologies). Data analysis was performed using FlowJo (Tree Star) software.

Cell sorting was performed using a FACSAria cell sorter (BD). Enrichment of Lin$^-$ cells was performed prior to cell sorting by negative magnetic selection using a MidiMACS Separator (Miltenyi Biotec). For this reason, cells were incubated with a lineage cocktail of biotinylated antibodies (Biotin-Conjugated Mouse Lineage Panel, BD Pharmingen) and subsequently with anti-Biotin MicroBeads (Miltenyi Biotec). To isolate endothelial cells, femurs and tibiae were crushed with a mortar and incubated for 30 minutes with collagenase type I (3 mg/ml, Life Technologies) prior to enrichment of Lin$^-$ cells. Endothelial cells were characterized as arteriolar endothelial cells (CD45$^-$Lin$^-$CD31$^+$Sca1$^+$) and sinusoidal endothelial cells (CD45$^-$Lin$^-$CD31$^+$Sca1$^-$). Cells were further characterized according to Vcam1 expression, as Vcam1^{hi} and Vcam1^{lo}.

For isolation of CXCL12-expressing niche cells, femurs were flushed and incubated with 1 U ml^{-1} liberase (Roche Applied Science) and 12 mU ml^{-1} DNase I (Sigma-Aldrich) in HBSS for 30 minutes at 37°C. Different subsets of CXCL12-expressing niche cells were identified by staining digested BM suspensions from *Cxcl12*^{GFP} reporter mice with biotinylated antibodies against TER-119 and CD45 (clone 30-F11; eBioscience), followed by incubation with streptavidin conjugated to DyLight 405 (Jackson ImmunoResearch Laboratories Inc.) and an anti-CD31 antibody (clone 390; eBioscience). High or intermediate levels of GFP in the CD45/TER119-negative fraction were used

to discriminate CAR cells ($CD45^-TER119^-CD31^-GFP^{hi}$), $CXCL12^+$endothelial cells ($CD45^-TER119^-CD31^+GFP^{int}$), and $CD31^-$ GFP^- mesenchymal stromal cells ($CD45^-TER119^-CD31^-GFP^-$) (33, 34). Cells were sorted on a FACSAria (BD Biosciences) to >95% purity.

For immunofluorescence, tibiae were collected and fixed for 2 hours in 4% paraformaldehyde. Bone decalcification was performed for 48 hours in Osteosoft (Merck Millipore), and bones were embedded in optical cutting temperature compound (OCT; Tissue-Tek). Endothelial cell staining in decalcified bones was performed using an APC-conjugated anti-CD31/PECAM-1 (clone 390; eBioscience) antibody and Alexa Fluor 694–conjugated anti-CD144/VE-cadherin (clone BV13; BioLegend), as described previously (7). In other experiments endothelial cell staining in bones was performed with a rat anti–mouse CD144/VE-cadherin (clone 11D4.1; BD Biosciences) antibody, followed by a goat anti-rat antibody conjugated with Alexa Fluor 647 (Thermo Fisher Scientific). In another set of experiments, staining of the vascular lumen was performed by administering an Alexa Fluor 594–conjugated Isolectin GS-IB_4 from *Griffonia simplicifolia* (Thermo Scientific), as described (75). Del-1 staining was performed with a rabbit anti–mouse Del-1 (Proteintech, catalog 12580-1-AP), followed by a goat anti-rabbit antibody conjugated with Alexa Fluor 488 (Thermo Scientific). Nuclear staining was performed with DAPI. Images were acquired with a Zeiss LSM 510 confocal microscope, an IX83 microscope equipped with a Yokogawa CSU-X1 spinning disc confocal scanner (Olympus), or a Nikon Eclipse Ni-E automated upright fluorescence microscope (Nikon).

Cell cycle analysis. For cell cycle analysis, BM cells were stained for cell surface markers as described in the previous paragraph, fixed using fixation/permeabilization buffer (eBioscience), and stained with anti–Ki-67 antibody. After washing, cells were stained with DAPI (Molecular Probes) and analyzed by flow cytometry.

Proteins. Del-1–Fc generation has been previously described (30). An RGE point mutant of Del-1–Fc, in which Glu (E) was substituted for Asp (D) in the RGD motif of the second EGF repeat (Del-1[RGE]–Fc), was constructed by site-directed mutagenesis (QuickChange II mutagenesis kit; Agilent). Expression and purification were performed as described (30).

Adhesion assay. Adhesion was performed as previously described with modifications (29, 76, 77). Nunc-Immuno MicroWell 96-well solid plates (Sigma-Aldrich) were coated overnight at 4°C with Del-1–Fc (10 μg/ml) and washed twice with PBS, and blockade was performed with 1% BSA in PBS for 1 hour. Sorted LSK cells were stained for 30 minutes with BCECF (1 μM, Life Technologies). After washing, cells were resuspended in HBSS supplemented with 2 μM Mn^{++} and incubated with 10 μg/ml rat IgG2a, κ isotype control (clone RTK2758; BioLegend), a rat IgG2b, κ isotype control (clone RTK4530; BioLegend), Armenian hamster IgG (clone HTK888; BioLegend), anti-CD11a (clone M17/4; BioLegend), anti-CD49d (clone R1-2; BioLegend), or anti-CD61 (clone 2C9.G2; BioLegend) for 15 minutes at 4°C. Cells were added to wells and incubated for 45 minutes at 37°C. Fluorescence was measured before (cell input) and after (adherent cells) washing, using a Synergy HT multi-mode microplate reader (Biotek Instruments). The percentage of adhesion is defined as the fluorescence of adherent cells divided by the fluorescence of cell input.

In vitro LSK cell incubation and Ccnd1 expression. Tissue culture 96-well plates (Greiner Bio-One) were coated overnight at 4°C with Del-1–Fc, Del-1[RGE]–Fc, or recombinant human IgG1 Fc (Fc-control; R&D Systems) (10 μg/ml each), as described under *Adhesion assay*. MyeloCult medium supplemented with stem cell factor (20 ng/ml, PeproTech) was used for the incubation of LSK cells. Isolated LSK cells were incubated for 3 hours to study the mRNA levels of *Ccnd1*. To inhibit ILK, LSK cells were treated with the ILK inhibitor Cpd22 (2 μM; Merck Millipore), whereas DMSO was used as control.

In vitro differentiation assay. Sorted LT-HSCs (500 cells per well), MPPs (1,000 cells per well), or CMPs (1,000 cells per well) were cultured in suspension culture 96-well plates (Greiner Bio-One) in MyeloCult medium supplemented with stem cell factor (20 ng/ml, PeproTech). Del-1–Fc, Del-1[RGE]–Fc, or recombinant human IgG1 Fc (Fc-control; R&D Systems) (500 ng/ml each) were added in the cultures. To inhibit β3 integrin, LT-HSCs were preincubated for 15 minutes before the addition of Del-1–Fc or Fc-control with cilengitide (25 μg/ml; Selleck Chemicals) or RGD control peptide (25 μg/ml; Enzo Life Sciences, GRADSP). After 48 hours or on day 7, the frequency of progenitor cells was analyzed by flow cytometry. The images from the colonies were acquired using a Zeiss Observer Z.1 inverted microscope.

Real-time PCR. For RNA isolation, cells were directly sorted into RNA isolation buffer, and RNA isolation was performed using an RNeasy Plus Micro Kit (QIAGEN), according to the manufacturer's instructions. RNA from the cBM and the endosteal region was collected using TRI reagent (Molecular Research Center Inc.), as previously described (5). Briefly, after repeatedly flushing the femurs into PBS supplemented with 5% FBS, for the isolation of cBM cells, the bones were flushed twice with TRI reagent to collect RNA from the endosteal region. RNA was reverse-transcribed with the iScript cDNA Synthesis Kit (Bio-Rad). Quantitative PCR was performed by using the SsoFast EvaGreen Supermix (BioRad) and gene-specific primers in a CFX384 Real-Time PCR Detection System (Bio-Rad). Relative mRNA expression levels were calculated according to the ΔΔCt method upon normalization to 18s or β2m for mouse samples and *GAPDH* for human samples.

CFU assay. CFU assay was performed using MethoCult GF M3434 medium (Stemcell Technologies), according to the manufacturer's instructions. Quantification of colony formation was performed using a STEMvision Instrument (Stemcell Technologies).

G-CSF measurement. G-CSF was measured in EDTA-plasma using a Mouse G-CSF DuoSet ELISA (R&D Systems), according to the manufacturer's instructions.

Statistics. All data are presented as mean ± SEM. Mann-Whitney *U* test was used for the comparison of two groups. In vitro comparison of matched groups was performed with a paired 2-tailed Student's *t* test. For comparisons of multiple groups, 1-way ANOVA followed by Holm-Šidák's multiple comparisons test was used. All statistical analysis was performed using GraphPad Prism 6 (GraphPad Software Inc.). Significance was set at $P < 0.05$.

Study approval. Animal experiments were approved by the Landesdirektion Sachsen, Germany; the Animal Care and Ethics Committee of the CNIC and regional authority of Madrid; and the Institutional Animal Care and Use Committee of the University of Pennsylvania. Primary human BM-derived MSCs (70, 72–74) were derived from BM aspirates from healthy donors after written informed consent was received and upon approval by the Ethics Committee of the Technische Universität Dresden.

Author contributions. IM designed the project, performed experiments, analyzed and interpreted data, and wrote the manuscript; LSC performed experiments and analyzed data; RPS performed experiments

and analyzed and interpreted data; IK, ME, TK, MT, AZ, KR, TM, TG, PS, and MDS performed experiments; KH and BW (Penn) generated critical reagents and interpreted data; MvB, MW, and MB provided human MSCs and interpreted data; PV, TT, and AH interpreted data; BW (Dresden) designed experiments, interpreted data, supervised research, and edited the manuscript; GH supervised research, interpreted data, and edited the manuscript; TC conceived and designed the project, interpreted data, supervised research, and wrote the manuscript.

Acknowledgments

The work was supported by the Deutsche Forschungsgemeinschaft (SFB 655–project B10 to TC); the European Community's Seventh Framework Program under grant agreement no. 602699 (to TC); the European Research Council (DEMETINL to TC); funding from the Excellence Initiative by the "German Federal and State Governments" (Institutional Strategy, measure "support the best" of the Technische Universität Dresden) to TC; and grants from the NIH (AI068730, DE024153, DE024716, and DE015254 to GH and DE026152 to GH and TC). The CNIC is supported by the MINECO and the Pro-CNIC Foundation, and is a Severo Ochoa Center of Excellence (MINECO award SEV-2015-0505). We thank S. Grossklaus, B. Gercken, and S. Galler for technical assistance.

Address correspondence to: Ioannis Mitroulis or Triantafyllos Chavakis, University Clinic Dresden, Fetscherstr. 74, 01307 Dresden, Germany. Phone: 49-351-458-19306; Email: Ioannis.Mitroulis@uniklinikum-dresden.de (I. Mitroulis). Phone: 49-351-458-6262; Email: Triantafyllos.Chavakis@uniklinikum-dresden.de (T. Chavakis).

TM's present address: Niigata University, Graduate School of Medical and Dental Sciences, Chuo-ku, Niigata, Japan.

1. Trumpp A, Essers M, Wilson A. Awakening dormant haematopoietic stem cells. *Nat Rev Immunol*. 2010;10(3):201–209.
2. Sun J, et al. Clonal dynamics of native haematopoiesis. *Nature*. 2014;514(7522):322–327.
3. Morrison SJ, Scadden DT. The bone marrow niche for haematopoietic stem cells. *Nature*. 2014;505(7483):327–334.
4. Kiel MJ, Yilmaz OH, Iwashita T, Yilmaz OH, Terhorst C, Morrison SJ. SLAM family receptors distinguish hematopoietic stem and progenitor cells and reveal endothelial niches for stem cells. *Cell*. 2005;121(7):1109–1121.
5. Winkler IG, et al. Vascular niche E-selectin regulates hematopoietic stem cell dormancy, self renewal and chemoresistance. *Nat Med*. 2012;18(11):1651–1657.
6. Itkin T, et al. Distinct bone marrow blood vessels differentially regulate haematopoiesis. *Nature*. 2016;532(7599):323–328.
7. Kunisaki Y, et al. Arteriolar niches maintain haematopoietic stem cell quiescence. *Nature*. 2013;502(7473):637–643.
8. Kusumbe AP, et al. Age-dependent modulation of vascular niches for haematopoietic stem cells. *Nature*. 2016;532(7599):380–384.
9. Ding L, Saunders TL, Enikolopov G, Morrison SJ. Endothelial and perivascular cells maintain haematopoietic stem cells. *Nature*. 2012;481(7382):457–462.
10. Acar M, et al. Deep imaging of bone marrow shows non-dividing stem cells are mainly perisinusoidal. *Nature*. 2015;526(7571):126–130.
11. Himburg HA, et al. Pleiotrophin regulates the retention and self-renewal of hematopoietic stem cells in the bone marrow vascular niche. *Cell Rep*. 2012;2(4):964–975.
12. Méndez-Ferrer S, et al. Mesenchymal and haematopoietic stem cells form a unique bone marrow niche. *Nature*. 2010;466(7308):829–834.
13. Mendelson A, Frenette PS. Hematopoietic stem cell niche maintenance during homeostasis and regeneration. *Nat Med*. 2014;20(8):833–846.
14. Kfoury Y, Scadden DT. Mesenchymal cell contributions to the stem cell niche. *Cell Stem Cell*. 2015;16(3):239–253.
15. Greenbaum A, et al. CXCL12 in early mesenchymal progenitors is required for haematopoietic stem-cell maintenance. *Nature*. 2013;495(7440):227–230.
16. Sugiyama T, Kohara H, Noda M, Nagasawa T. Maintenance of the hematopoietic stem cell pool by CXCL12-CXCR4 chemokine signaling in bone marrow stromal cell niches. *Immunity*. 2006;25(6):977–988.
17. Silberstein L, et al. Proximity-based differential single-cell analysis of the niche to identify stem/progenitor cell regulators. *Cell Stem Cell*. 2016;19(4):530–543.
18. Lo Celso C, et al. Live-animal tracking of individual haematopoietic stem/progenitor cells in their niche. *Nature*. 2009;457(7225):92–96.
19. Doan PL, et al. Epidermal growth factor regulates hematopoietic regeneration after radiation injury. *Nat Med*. 2013;19(3):295–304.
20. Himburg HA, et al. Pleiotrophin regulates the expansion and regeneration of hematopoietic stem cells. *Nat Med*. 2010;16(4):475–482.
21. To LB, Levesque JP, Herbert KE. How I treat patients who mobilize hematopoietic stem cells poorly. *Blood*. 2011;118(17):4530–4540.
22. Peffault de Latour R, et al. Recommendations on hematopoietic stem cell transplantation for inherited bone marrow failure syndromes. *Bone Marrow Transplant*. 2015;50(9):1168–1172.
23. Gertz MA. Current status of stem cell mobilization. *Br J Haematol*. 2010;150(6):647–662.
24. Morgan SJ, et al. Predictive factors for successful stem cell mobilization in patients with indolent lymphoproliferative disorders previously treated with fludarabine. *Leukemia*. 2004;18(5):1034–1038.
25. Bennett CL, Djulbegovic B, Norris LB, Armitage JO. Colony-stimulating factors for febrile neutropenia during cancer therapy. *N Engl J Med*. 2013;368(12):1131–1139.
26. Smith TJ et al. Recommendations for the use of WBC growth factors: American Society of Clinical Oncology Clinical Practice Guideline Update. *J Clin Oncol*. 2015;33(28):3199–3212.
27. Donini M, et al. G-CSF treatment of severe congenital neutropenia reverses neutropenia but does not correct the underlying functional deficiency of the neutrophil in defending against microorganisms. *Blood*. 2007;109(11):4716–4723.
28. Dale DC, et al. Severe chronic neutropenia: treatment and follow-up of patients in the Severe Chronic Neutropenia International Registry. *Am J Hematol*. 2003;72(2):82–93.
29. Choi EY, et al. Del-1, an endogenous leukocyte-endothelial adhesion inhibitor, limits inflammatory cell recruitment. *Science*. 2008;322(5904):1101–1104.
30. Shin J, et al. DEL-1 restrains osteoclastogenesis and inhibits inflammatory bone loss in nonhuman primates. *Sci Transl Med*. 2015;7(307):307ra155.
31. Eskan MA, et al. The leukocyte integrin antagonist Del-1 inhibits IL-17-mediated inflammatory bone loss. *Nat Immunol*. 2012;13(5):465–473.
32. Hajishengallis G, Chavakis T. Endogenous modulators of inflammatory cell recruitment. *Trends Immunol*. 2013;34(1):1–6.
33. Casanova-Acebes M, et al. Rhythmic modulation of the hematopoietic niche through neutrophil clearance. *Cell*. 2013;153(5):1025–1035.
34. Leiva M, Quintana JA, Ligos JM, Hidalgo A. Haematopoietic ESL-1 enables stem cell proliferation in the bone marrow by limiting TGFβ availability. *Nat Commun*. 2016;7:10222.
35. Maekawa T, et al. Antagonistic effects of IL-17 and D-resolvins on endothelial Del-1 expression through a GSK-3β-C/EBPβ pathway. *Nat Commun*. 2015;6:8272.
36. Lai AY, Kondo M. Asymmetrical lymphoid and myeloid lineage commitment in multipotent hematopoietic progenitors. *J Exp Med*. 2006;203(8):1867–1873.
37. Pietras EM, et al. Functionally distinct subsets of lineage-biased multipotent progenitors control blood production in normal and regenerative conditions. *Cell Stem Cell*. 2015;17(1):35–46.
38. Yang L, et al. Identification of Lin(-)Sca1(+)kit(+)CD34(+)Flt3- short-term hematopoietic stem cells capable of rapidly reconstituting and rescuing myeloablated transplant recipients. *Blood*. 2005;105(7):2717–2723.
39. Xie Y, et al. Detection of functional haematopoietic stem cell niche using real-time imaging. *Nature*. 2009;457(7225):97–101.
40. Busch K, et al. Fundamental properties of unperturbed haematopoiesis from stem cells in vivo.

Nature. 2015;518(7540):542–546.
41. Wilson A, et al. Hematopoietic stem cells reversibly switch from dormancy to self-renewal during homeostasis and repair. *Cell*. 2008;135(6):1118–1129.
42. Passegué E, Wagers AJ, Giuriato S, Anderson WC, Weissman IL. Global analysis of proliferation and cell cycle gene expression in the regulation of hematopoietic stem and progenitor cell fates. *J Exp Med*. 2005;202(11):1599–1611.
43. Bowie MB, McKnight KD, Kent DG, McCaffrey L, Hoodless PA, Eaves CJ. Hematopoietic stem cells proliferate until after birth and show a reversible phase-specific engraftment defect. *J Clin Invest*. 2006;116(10):2808–2816.
44. Mettouchi A, et al. Integrin-specific activation of Rac controls progression through the G(1) phase of the cell cycle. *Mol Cell*. 2001;8(1):115–127.
45. Streuli CH. Integrins and cell-fate determination. *J Cell Sci*. 2009;122(Pt 2):171–177.
46. Umemoto T, et al. Integrin-αvβ3 regulates thrombopoietin-mediated maintenance of hematopoietic stem cells. *Blood*. 2012;119(1):83–94.
47. Umemoto T, et al. Expression of Integrin beta3 is correlated to the properties of quiescent hemopoietic stem cells possessing the side population phenotype. *J Immunol*. 2006;177(11):7733–7739.
48. Papayannopoulou T, Craddock C, Nakamoto B, Priestley GV, Wolf NS. The VLA4/VCAM-1 adhesion pathway defines contrasting mechanisms of lodgement of transplanted murine hemopoietic progenitors between bone marrow and spleen. *Proc Natl Acad Sci USA*. 1995;92(21):9647–9651.
49. Chen C, Liu Y, Liu Y, Zheng P. Mammalian target of rapamycin activation underlies HSC defects in autoimmune disease and inflammation in mice. *J Clin Invest*. 2010;120(11):4091–4101.
50. Nagai Y, et al. Toll-like receptors on hematopoietic progenitor cells stimulate innate immune system replenishment. *Immunity*. 2006;24(6):801–812.
51. Zhao JL, et al. Conversion of danger signals into cytokine signals by hematopoietic stem and progenitor cells for regulation of stress-induced hematopoiesis. *Cell Stem Cell*. 2014;14(4):445–459.
52. Boettcher S, et al. Endothelial cells translate pathogen signals into G-CSF-driven emergency granulopoiesis. *Blood*. 2014;124(9):1393–1403.
53. Boettcher S, et al. Cutting edge: LPS-induced emergency myelopoiesis depends on TLR4-expressing nonhematopoietic cells. *J Immunol*. 2012;188(12):5824–5828.
54. Manz MG, Boettcher S. Emergency granulopoiesis. *Nat Rev Immunol*. 2014;14(5):302–314.
55. Morrison SJ, Wright DE, Weissman IL. Cyclophosphamide/granulocyte colony-stimulating factor induces hematopoietic stem cells to proliferate prior to mobilization. *Proc Natl Acad Sci USA*. 1997;94(5):1908–1913.
56. Schuettpelz LG, et al. G-CSF regulates hematopoietic stem cell activity, in part, through activation of Toll-like receptor signaling. *Leukemia*. 2014;28(9):1851–1860.
57. Semerad CL, et al. G-CSF potently inhibits osteoblast activity and CXCL12 mRNA expression in the bone marrow. *Blood*. 2005;106(9):3020–3027.
58. Lévesque J-P, Hendy J, Takamatsu Y, Simmons PJ, Bendall LJ. Disruption of the CXCR4/CXCL12 chemotactic interaction during hematopoietic stem cell mobilization induced by GCSF or cyclophosphamide. *J Clin Invest*. 2003;111(2):187–196.
59. Nakamura-Ishizu A, et al. Extracellular matrix protein tenascin-C is required in the bone marrow microenvironment primed for hematopoietic regeneration. *Blood*. 2012;119(23):5429–5437.
60. Yu VWC et al. Epigenetic memory underlies cell-autonomous heterogeneous behavior of hematopoietic stem cells. *Cell*. 2016;167(5):1310–1322.e17.
61. Yang J, et al. Single cell transcriptomics reveals unanticipated features of early hematopoietic precursors. *Nucleic Acids Res*. 2017;45(3):1281–1296.
62. Kozar K et al. Mouse development and cell proliferation in the absence of D-cyclins. *Cell*. 2004;118(4):477–491.
63. Zhu X, Ohtsubo M, Böhmer RM, Roberts JM, Assoian RK. Adhesion-dependent cell cycle progression linked to the expression of cyclin D1, activation of cyclin E-cdk2, and phosphorylation of the retinoblastoma protein. *J Cell Biol*. 1996;133(2):391–403.
64. Wang YH, et al. Cell-state-specific metabolic dependency in hematopoiesis and leukemogenesis. *Cell*. 2014;158(6):1309–1323.
65. Choi EY, et al. Developmental endothelial locus-1 is a homeostatic factor in the central nervous system limiting neuroinflammation and demyelination. *Mol Psychiatry*. 2015;20(7):880–888.
66. Miller PG, et al. In vivo RNAi screening identifies a leukemia-specific dependence on integrin beta 3 signaling. *Cancer Cell*. 2013;24(1):45–58.
67. Bruns I, et al. Megakaryocytes regulate hematopoietic stem cell quiescence through CXCL4 secretion. *Nat Med*. 2014;20(11):1315–1320.
68. Purton LE, Scadden DT. Limiting factors in murine hematopoietic stem cell assays. *Cell Stem Cell*. 2007;1(3):263–270.
69. Kim K-H, Chen C-C, Alpini G, Lau LF. CCN1 induces hepatic ductular reaction through integrin αvβ5–mediated activation of NF-κB. *J Clin Invest*. 2015;125(5):1886–1900.
70. Oswald J, et al. Mesenchymal stem cells can be differentiated into endothelial cells in vitro. *Stem Cells Dayt*. 2004;22(3):377–384.
71. von Dalowski F, et al. Mesenchymal stromal cells for treatment of acute steroid-refractory graft versus host disease: clinical responses and long-term outcome. *Stem Cells*. 2016;34(2):357–366.
72. Dhawan A, et al. Breast cancer cells compete with hematopoietic stem and progenitor cells for intercellular adhesion molecule 1-mediated binding to the bone marrow microenvironment. *Carcinogenesis*. 2016;37(8):759–767.
73. Duryagina R, et al. Overexpression of Jagged-1 and its intracellular domain in human mesenchymal stromal cells differentially affect the interaction with hematopoietic stem and progenitor cells. *Stem Cells Dev*. 2013;22(20):2736–2750.
74. Wobus M, et al. Breast carcinoma cells modulate the chemoattractive activity of human bone marrow-derived mesenchymal stromal cells by interfering with CXCL12. *Int J Cancer*. 2015;136(1):44–54.
75. Nombela-Arrieta C, et al. Quantitative imaging of haematopoietic stem and progenitor cell localization and hypoxic status in the bone marrow microenvironment. *Nat Cell Biol*. 2013;15(5):533–543.
76. Choi EY, et al. Regulation of LFA-1-dependent inflammatory cell recruitment by Cbl-b and 14-3-3 proteins. *Blood*. 2008;111(7):3607–3614.
77. Chung KJ, et al. A self-sustained loop of inflammation-driven inhibition of beige adipogenesis in obesity. *Nat Immunol*. 2017;18(6):654–664.